VEQTER Ltd. 78 Queens Road, Clifton, Bristol, BS8 1QU, UK
t +44 (0) 117 985 8742 f +44 (0) 117 985 6971 e experts@veqter.co.uk w www.veqter.co.uk

Residual VEQTER Stress Experts

Client:

POSIVA

Report No.: R11-001 – Version 3

Project Title:

DHD residual stress measurements within the cast iron insert of a radioactive waste canister

Authors:

D. A. Bowman and E. J. Kingston

13th December 2013

CONTENTS

1 INTRODUCTION

VEQTER Ltd was requested by POSIVA under quotation purchase order 9388-11 (1) to undertake a number of residual stress measurements using the Deep-Hole Drilling (DHD) technique. This report provides details of the measurements carried out for this order, namely the measurement of bi-axial residual stresses using the DHD technique in the cast iron insert of a radioactive waste canister supplied by POSIVA.

2 SPECIMEN DESIGN

POSIVA supplied a single specimen to VEQTER Ltd's facilities in the UK. The specimen was a section of cast iron insert I63 designed to house spent radioactive BWR fuels in a final disposal canister, as photographed in Figure 1. The section was cut from about 1310 – 2290 mm from the bottom of the complete insert. The final canister structure consisted of a cylindrical, nodular graphite, cast iron insert covered by a 50 mm thick copper overlay. However, the measurements described in this report were made prior to final machining and insertion into the copper.

The cast iron insert was 960 mm in diameter, roughly 980 mm in length and was predominantly made from nodular graphite cast iron. The proposed quality was EN-GJS-400-15U according to the European standard SFS-EN 1563. The minimum ultimate strength according to the standard is 370 MPa. The steel tubes (180 mm square with a 10 mm wall thickness) within the insert were made of structural steel S355J2G3 with an ultimate tensile strength of 490 - 630 MPa (1).

3 DEEP-HOLE DRILLING PROCEDURE

The DHD residual stress measurement technique is a semi-invasive, mechanical strain relief technique (i.e. the strain of the component is measured during stress relief from the removal of a small amount of material). The procedure used for the DHD technique can be divided into 5 stages (2), as shown in Figure 2 for a simple welded component:

1. Reference bushes are attached to the front and back surfaces of the component at the measurement location.

2. A 1.5 mm or 3 mm diameter reference hole is gundrilled through the component and reference bushes.

3. The diameter, $Ø_0$, of the reference hole is measured through the entire thickness of the component and reference bushes using an air-probe. Diameter measurements are taken at 0.2 mm increments in depth and at 22.5 º increments in angle about the axis of the reference hole.

4. A cylinder (i.e. core) of material, containing the reference hole along its axis is cut from the component using electro-discharge machining (EDM).

5. The diameter, Ø, of the reference hole is re-measured through the entire thickness of the cylinder and reference bushes. Diameter measurements are taken at the same locations as those measured in Stage 3.

The diameter, $Ø_0$, of the reference hole measured in Stage 3 is the diameter when stresses are present. During Stage 4 the stresses are relieved, hence the diameter, Ø, of the reference hole measured in Stage 5 is the diameter when stresses are not present. The differences between the measured diameters in Stages 3 and 5 enable the original residual stresses to be calculated.

Technique Accuracy:

Because the technique measures diameters at Stage 3 and Stage 5 through the thickness of the specimen, a true stress profile can be generated without the need for material response coefficients as with most mechanical strain relaxation techniques. Therefore the measurement accuracy is independent of depth and specimen thickness.

Although the DHD technique is indifferent to the surface finish of the component, there are surface phenomena that affect the accuracy of shallow measurements, or measurements near a free surface. The bushes applied in Stage 1 of the DHD procedure described above minimise most of the experimental equipment errors that occur near the entrance and exit of the specimen during the DHD technique, e.g. bell-mouthing of the reference hole and air-probe air flow effects. However elasticity surface effects also occur at these surfaces that alter the shape of the reference hole (3). Due to the difficulty in incorporating these effects, which can only be accounted for using modelled coefficients, some DHD surface results have been omitted. All the results submitted in this report are accurate to the detailed uncertainty analysis of the DHD technique published by Goudar et al (4). In this paper different approaches leading to the evaluation of uncertainties were discussed, however, for practical purposes only the uncertainty based on the propagation of errors was considered. The errors currently presented for the measurements undertaken comprise of:

1. Calibration Error – due to a combination of human and instrument error in the calibration of the air probe before and after measuring the hole diameter.
2. Curve-fit Error – due to the curve fitting of the air probe calibration data.
3. Misalignment Error – accounting for surface roughness of the reference hole and the core extension.
4. Material Constant – Young's modulus error – generally a 5 % uncertainty is assumed unless the data provided by the client informs us otherwise.

The above parameters contain the major sources of uncertainty in the measured residual stresses using the DHD technique. However, other sources of uncertainty, including; plasticity effects, exclusion of the third strain component, effects of the 2θ 'strain fit' calculations and the analytical assumption of independent block lengths of material are difficult to characterise and therefore not included, but nevertheless they are thought to be relatively negligible. The uncertainty due to air-probe angular misalignment presented by Goudar et al (4) using random number analysis cannot be obtained via experiment and hence is also not included. However, based on the random number analysis, uncertainty due to angular misalignment is negligible compared to the other sources of uncertainty.

4 MEASUREMENT LOCATIONS

There were six DHD measurements made in total in the cast iron insert specimen. Five of the measurements were contracted, whilst one was the result of an incorrect measurement location and is presented in the report for your interest but is surplus to requirements. Each measurement

location was defined by POSIVA, as shown in Figure 3, and then drilled along the prescribed line at a suitable distance from the specimen end surface. It was agreed with POSIVA to perform the measurements shown in Figure 3 in different quadrants of the specimen as long as they were representative of those defined in Figure 3 (1). This was carried out to keep the manipulation of the heavy specimen to a minimum and the final measurement locations in the specimen are shown in Figure 4. The distances from the measurements to the cut ends were kept as large as possible to avoid the effects the free surfaces may have on the residual stress field. However, the locations were spread across the specimen's entire length to allow access to apply bushes and to fit as many measurements as possible in a single quadrant.

The location marked "incorrect measurement" was not prescribed by POSIVA and was a result of an incorrect attempt at measurement 4. In the case of locations 1, 2 and 3 the measurements were made radially towards the centre of the specimen, thus the in plane stresses normal to the measurement lines are the axial and hoop stresses. In the case of measurements 4 and 5 the measurements were not made radially and as such the in-plane stresses normal to the measurement lines are axial and a combination of hoop and radial stress directions. Throughout this report these hoop-radial combinations will be referred to as 'hoop' for simplicity.

Measurement 1:

The measurement at this location was made, as prescribed by POSIVA, to penetrate the corner of an outer steel tube whilst being drilled radially inward towards the specimen axis. This location was 300 mm from the end surface (shown in Figure 4) of the specimen. Due to the short length of the measurement a 1.5 mm diameter reference hole was drilled, with a 5 mm diameter core cut from the specimen. The gundrilling procedure was successful, and left a reference hole with an average diameter of 1.5006 mm with a standard deviation of 0.0028 mm. The EDM stress relief procedure was also successful, removing cast iron and steel tube cores with lengths of approximately 39 mm and 10 mm, as seen in Figure 5. Figure 6 shows the DHD machine set to the specimen as used for all the stages of the DHD process.

Measurement 2:

The measurement at this location was made, as prescribed by POSIVA, to penetrate the corner of an inner steel tube whilst being drilled radially inwards towards the specimen axis. This location was 315 mm from the end surface (shown in Figure 4) of the specimen. Due to the large measurement depth required at this location a 3 mm diameter reference hole was drilled and a 10 mm diameter core was cut from the specimen. The gundrilling procedure was successful and left a reference hole with an average diameter of 3.0041 mm with a standard deviation of 0.0041 mm. The EDM stress relief procedure was also successful, removing cast iron and steel tube cores with lengths of approximately 216 mm and 10 mm, as seen in Figure 7.

Measurement 3:

The measurement at this location was made, as prescribed by POSIVA, to avoid the steel tubes and penetrate radially inwards through the specimen axis. As this location was a 'blind hole' no reference bush was applied to the back of the specimen. This location was 487 mm from the

end surface (shown in Figure 4) of the specimen. Again, due to the depth of measurement at this location a 3 mm diameter reference hole was drilled and a 10 mm diameter core was trepanned into the specimen. The gundrilling procedure was successful, and left a reference hole with an average diameter of 2.9986 mm with a standard deviation of 0.0018 mm. The EDM stress relief procedure was also successful. However, as the measurement was not performed completely through the specimen, the core was not extracted and so remains attached to the specimen.

Measurement 4:

The measurement at this location was made, as prescribed by POSIVA, to penetrate the corner of an outer steel tube, but travelling parallel to the tube wall and along the wall centreline. This location was 677 mm from the end surface (shown in Figure 4) of the specimen. At this location a 3 mm diameter reference hole was drilled and a 10 mm diameter core was trepanned into the specimen. The gundrilling procedure was successful, and left a reference hole with an average diameter of 2.9938 mm with a standard deviation of 0.0014 mm. The EDM stress relief procedure was also successful. However, as the measurement was not performed completely through the specimen, the core was not extracted and so remains attached to the specimen.

Measurement 5:

The measurement at this location was made, as prescribed by POSIVA, to penetrate from the inner corner of an outer steel tube diagonally through the cast iron to the outer corner of an inner steel tube. Prior to the measurement, material was removed between the outer surface of the cast iron and the outside corner of an outer steel tube. This allowed access to the inner corner of the outer tube and diagonally through to the wall of the inner tube. This location was 302 mm from the end surface (shown in Figure 4) of the specimen. At this location a 3 mm diameter reference hole was drilled and a 10 mm diameter core was cut from the specimen. The gundrilling procedure was successful, and left a reference hole with an average diameter of 2.9962 mm with a standard deviation of 0.0007 mm. The EDM stress relief procedure was also successful, removing cast iron and steel tube cores with lengths of approximately 63 mm and 10 mm as seen in Figure 8.

Incorrect Measurement:

The measurement at this location was intended to be measurement 4, but was incorrectly located and so now surplus to those dictated by POSIVA. As such the measurement line penetrated the corner of an outer steel tube, but travelled parallel to the tube wall and was aligned to the wall centreline. The measurement was at a similar location to measurement 1, but drilled parallel to the tube wall, not radially. At this location measurements were already carried out through the cast iron section before the mistake was realised and so only cast iron measurements are presented. This location was 302 mm from the end surface of the specimen. At this location a 3 mm reference hole was drilled and a 10 mm core was trepanned into the specimen. The gundrilling procedure was successful, and left a reference hole with an average diameter of 2.9922 mm with a standard deviation of 0.0019 mm. The EDM stress relief procedure was also successful. However, as the measurement was not performed completely through the specimen, the complete core was not extracted.

5 RESULTS AND DISCUSSION

Under this work scope only the in-plane distortions of the reference holes were measured following stress relief. The distortions were then converted into residual stresses using a Young's modulus, *E*, of 166 GPa for the cast iron and 210 GPa for the steel tubes (1). The analysis used to convert the measured distortions into stresses assumes isotropic, plane stress conditions and as such the Poisson's ratio was not required. Figure 6 and Figure 9 show the DHD machine setups on the specimen during gundrilling and air probing respectively, with the orientation of axes for the axial, hoop or 'hoop' and shear directions illustrated.

The in-plane through-thickness residual stresses measured using the DHD technique in the cast iron insert specimen at measurement locations 1 to 6 are recorded in Table 1 to Table 6 and illustrated in Figure 10 to Figure 15. Each of the measured stress directions is plotted as a function of depth from the surface at which the gundrilling process began. In this report a reduced data set has been supplied, giving measurements at 1 mm depth increments as opposed to 0.2 mm increments in order to reduce table size. Where the cores have separated into separate iron and steel sections they have been measured and analysed separately, as if separate components. As a result measurement data is not provided 1 mm from each separate free surface due to surface effects as previously discussed.

Measurement 1:

The residual stresses measured at this location using the DHD technique are recorded in Table 1 and illustrated in Figure 10. The axial and hoop residual stresses were found to follow similar profiles in the cast iron, but differ in the steel tube. Neither the hoop nor the axial stresses were dominant in the cast iron, whereas the axial stresses were higher in the steel tube. Through much of the cast iron section the fluctuations of the axial and hoop stress profiles are below the accuracy of the DHD technique and as such are not described. The axial and hoop mean error values for this measurement were both ±18 MPa, with standard deviations of 3 MPa and 2 MPa respectively.

The axial residual stresses were found to start at approximately 10 MPa at the outer cast iron surface, before increasing sharply to a maximum tensile value in the cast iron of 58 MPa at 2 mm. From here they fluctuated whilst decreasing slowly, into compression, to reach a minimum value at the cast iron/steel tube interface of -34 MPa at 37.8 mm deep. The steel tube measurement starts at 39.8 mm from the outer surface with an initial axial residual stress level of 116 MPa. From here the axial stresses increased to a peak of 118 MPa at 40.4 mm before decreasing to 96 MPa at 42.8 mm. They then increased again to 114 MPa at 45 mm before decreasing to a minimum value in the steel of 93 MPa at 47.8 mm, approximately 1 mm from the inner surface of the steel tube.

The hoop residual stresses were found to start at approximately 25 MPa at the outer cast iron surface, before increasing sharply to a maximum tensile value in the cast iron of 57 MPa at 1.8 mm. From here they fluctuated whilst decreasing slowly, into compression, to reach a minimum value at the cast iron/steel tube interface of -60 MPa 37.8 mm deep. The steel tube begins with an initial hoop residual stress level of 47 MPa. From here the hoop stresses increased to 51 MPa at 40.2 mm before decreasing to a minimum value in the steel of 18 MPa at 43.4 mm. They then increased again to 64 MPa at 47 mm before decreasing to 49 MPa at 47.8 mm, approximately 1 mm from the inner surface of the steel tube.

The resolved shear stresses also fluctuated throughout the cast iron, with an average value of -3 MPa and a standard deviation of 7 MPa and showing maximum and minimum values of 20 MPa and -15 MPa at 37.8 mm and 33.4 mm respectively. Alternatively in the steel tube section, the shear stresses remained more constant with an average value of -10 MPa and a standard deviation of just 2 MPa.

Measurement 2:

The residual stresses measured at this location using the DHD technique are recorded in Table 2 and shown in Figure 11. The axial and hoop stresses show similar shapes, but different magnitudes in both the cast iron and the steel tube sections. Neither the hoop nor the axial stresses were dominant in the cast iron, whereas the axial stresses were generally higher in the steel tube. Through much of the cast iron section the fluctuations of the axial and hoop stress profiles were below the accuracy of the DHD technique and as such are not described. The axial and hoop mean error values for this measurement are both ±13 MPa, with standard deviations of 3 MPa and 2 MPa respectively.

The axial residual stresses were found to start at a peak compressive value of approximately -62 MPa at the outer cast iron surface, before increasing sharply to a maximum tensile value in the cast iron of 4 MPa at 5.4 mm. From here they fluctuated within the error bounds of the measurement, reaching the cast iron/steel tube interface at -5.1 MPa, 212.4 mm deep. The axial residual stresses in the steel tube were found to start at 35 MPa at 214.6 mm, increasing sharply to a peak of 72 MPa at 218.8 mm. From here they then decreased to 15 MPa at 222.6 mm deep, approximately 1 mm from the steel tube inner surface.

The hoop residual stresses were found to start at approximately -41 MPa at the outer cast iron surface, before increasing sharply to 11 MPa at 5.4 mm. From here they fluctuated within the error bounds of the measurement, averaging 12 MPa higher than the axial stress levels, reaching a maximum value of 17 MPa at 18.6 mm and finishing at the cast iron/steel tube interface at 2.3 MPa at 212.4 mm deep. The hoop residual stresses in the steel tube were found to start at a minimum value of -61 MPa at 214.6 mm and increased sharply to a peak of 16 MPa at 220 mm. From here the hoop stresses then decreased again to 1 MPa at 222.6 mm deep, approximately 1 mm from the steel tube inner surface.

The resolved shear residual stresses remained low throughout the cast iron, with an average value of 0 MPa and a standard deviation of 1.8 MPa. However in the steel tube section, the shear stresses started at the cast iron/steel tube interface with a peak of 11 MPa, before decreasing to 1 MPa at 217 mm and remaining more constant for the remainder of the steel tube thickness, with an average value of 4 MPa and a standard deviation of 2 MPa for the steel insert section.

Measurement 3:

The residual stresses measured at this location using the DHD technique are recorded in Table 3 and shown in Figure 12. The axial and hoop stresses show fairly similar profiles with the hoop stresses slightly more tensile for the majority of measurement depths. Neither the hoop nor the axial stresses were dominant in the cast iron and through much of the cast iron section the features of the axial and hoop stress profiles were below the accuracy of the DHD technique

and as such are not described. The axial and hoop mean error values for this measurement were both ±11 MPa with a standard deviation of 1MPa

The axial residual stresses were found to start at a peak compressive value of approximately -113 MPa at the outer cast iron surface, before increasing sharply to -14 MPa at 20 mm. They fluctuated around -14 MPa for a further 80 mm reaching -7 MPa at 100 mm at which point the axial stresses increased slightly to fluctuate around approximately 0 MPa for a further 140 mm to reach -1 MPa at 240 mm. At this point they increased again to around 10 MPa at 273.8 mm and they continued to fluctuate around this value until the last measurement point of 5 MPa at 512 mm, slightly past the centre point of the specimen.

The hoop residual stresses were found to start at a compressive peak of approximately -81 MPa at the outer cast iron surface, before increasing sharply to 0 MPa at 21.4 mm. The hoop stresses remained low for approximately 220 mm, fluctuating slightly above zero and reaching 5 MPa at 242 mm. From here they increased slightly to a maximum tensile peak of 25 MPa at 277 mm before decreasing back to approximately 10 MPa at 320 mm. They fluctuate around this value for a further 120 mm to 440 mm deep at which point they increase to a second tensile peak of 22 MPa at 465 mm. After this the hoop residual stresses reduced to reach 3 MPa at the final measurement point at 512 mm deep.

The resolved shear residual stresses remained low throughout the cast iron at an average of -2 MPa with a standard deviation of 2 MPa.

Measurement 4:

The residual stresses measured at this location using the DHD technique are recorded in Table 4 and illustrated in Figure 13. The axial and 'hoop' residual stresses were found to follow similar profiles in the cast iron, but differ in the steel tube. Neither the axial nor the 'hoop' stresses were dominant in the cast iron, whereas the axial stresses were higher in the steel tube. At this location the measurement direction was not radially inwards towards the specimen axis so the 'hoop' stresses have a small radial stress component within them. Once in the steel tube the 'hoop' stress direction is equivalent to the steel tube wall transverse direction. For this measurement the angle between the measurement axis and the cast iron/steel tube interface plane was at its greatest. This caused technical difficulties both gundrilling and air probing which resulted in approximately 6 mm of measurement data being omitted due to uncertainty. The axial and 'hoop' mean error values for this measurement were ±12 MPa and ±13 MPa respectively, both with standard deviations of 1 MPa.

The axial residual stresses were found to start with a compressive value of -38 MPa at the outer cast iron surface, before increasing into tension to a maximum tensile value in the cast iron of 12 MPa at 8.8 mm. They then decrease again into compression to reach -16 MPa at 22.0 mm deep. The axial residual stresses then fluctuated around this level until 79 mm deep at which point they decreased further into compression to reach a maximum compressive value of -39 MPa at 84.4 mm at which point the cast iron measurement finishes. The steel tube measurement started with a minimum value of 55 MPa at 91.2 mm from the outer cast iron surface before rising to a maximum tensile value of 69 MPa at 97 mm. From here they decreased slightly to 67 MPa at 103 mm, the last measurement point in the steel tube section.
The 'hoop' residual stresses were found to start with a maximum compressive value of -35 MPa at the outer cast iron surface, before increasing into tension to a maximum tensile value in the

cast iron of 6 MPa at 8.8 mm. They then decreased again into compression to reach -23 MPa at 24.4 mm deep. The 'hoop' residual stresses then increase slowly to -2 MPa at 76 mm, at which point they decrease again to reach a compressive value of -34 MPa at 84.4 mm for the final cast iron measurement point. The steel tube measurement started with a maximum compressive value of -43 MPa at 91.2 mm from the outer cast iron surface before rising sharply to -18 MPa at 93 mm. From here they increased more slowly to reach a maximum 'hoop' stress value of -11 MPa at 103 mm, the last measurement point in the steel tube section.

The resolved shear stresses only fluctuated slightly throughout the cast iron, with an average value of -6 MPa and a standard deviation of 1 MPa. Alternatively in the steel tube section, the shear stresses increased from the outside surface to the inside surface, starting at -5 MPa at 91.2 mm and finishing at 5 MPa at 103 mm.

Measurement 5:

The residual stresses measured at this location using the DHD technique are recorded in Table 5 and illustrated in Figure 14. The axial and 'hoop' residual stresses were found to differ in both the steel tube sections and the cast iron sections, with axial stresses greater in the steel tubes and hoop stresses greater in the cast iron. At this location the measurement direction was not radially inwards towards the specimen axis and the reported 'hoop' stresses have an equal hoop and radial stress component in them. The measurement started in a steel tube, moved into the cast iron and then exited through another steel tube, as such there were two cast iron/steel tube interfaces. The axial and 'hoop' mean error values for this measurement were both ±21 MPa with a standard deviation of 3 MPa.

The axial residual stresses were found to start with a tensile value of 51 MPa at the inner surface of the outer steel tube, before increasing to a maximum tensile value of 88 MPa at 4.6 mm. They then decreased to 66 MPa at the first cast iron/steel tube interface at 9.2 mm deep. The axial residual stresses then remained fairly constant during the cast iron section, starting at a peak compressive value of -20 MPa at 11.4 mm, but quickly rising to -2 MPa at 14.2 mm and fluctuating around zero for the remaining cast iron section until the last cast iron measurement at 72.4 mm. The axial stresses within the second steel tube started at 56 MPa at 74.6 mm before rising to a maximum value of 71 MPa at 80.2 mm. From here they decreased to 31 MPa at 83.2 mm, the last measurement point within the second steel tube section.

The 'hoop' residual stresses were found to start at 39 MPa at the inner surface of the outer steel tube, increasing slightly to a maximum tensile value of 41 MPa at 3 mm, before decreasing to approximately 0 MPa at the first cast iron/steel tube interface at 9.2 mm deep. The 'hoop' residual stresses then remained fairly constant during the cast iron section, starting at 25 MPa at 11.4 mm, decreasing to 16 MPa at 36.4 mm before increasing again to a maximum 'hoop' stress in the cast iron of 34 MPa at 66.4 mm. They then decreased slightly to 24 MPa for the last cast iron measurement at 72.4 mm deep. The 'hoop' stresses within the second steel tube started at 4 MPa at 74.6 mm deep before rising to a maximum value of 41 MPa at 80.2 mm. From here they decreased again to 37 MPa at 83.2 mm, the last measurement point within the second steel tube section.

The resolved shear stresses only fluctuated slightly throughout the cast iron, with an average value of 1 MPa and a standard deviation of 2 MPa. Alternatively in both the steel tube sections, the shear stresses increased with the depth of the measurement. In the first steel tube section the

resolved shear stresses started at -28 MPa, increasing to -5 MPa at the cast iron/steel tube interface. In the second steel tube the shear stresses increased from -18 MPa at the cast iron/steel tube interface at 74.6 mm deep to 9 MPa at the inner steel tube inner surface at 83.2 mm deep.

Incorrect Measurement:

The residual stresses measured at this location using the DHD technique are recorded in Table 6 and illustrated in Figure 15. For this measurement only the cast iron values are presented as the trepanning process was not continued into the steel tube. The axial and 'hoop' residual stresses were found to follow similar profiles throughout the cast iron and as such neither stress direction was dominant. At this location the measurement direction was not radially inwards toward the centre so the 'hoop' stresses are again a combination of the hoop and radial directions. The axial and 'hoop' stress mean error values for this measurement were found to be ±12 MPa and ±13 MPa respectively with standard deviations of 1 MPa and 4 MPa respectively.

The axial residual stresses were found to start with a maximum compressive value of -59 MPa at the outer cast iron surface, before increasing into tension to a maximum tensile value of 34 MPa at 5.0 mm. They then decreased gradually into compression to reach -11 MPa at 23.8 mm deep. The axial residual stresses then fluctuated around this level finishing at -4 MPa at the cast iron/steel tube interface at 46.8 mm deep.

The 'hoop' residual stresses were found to start with a maximum compressive value of -32 MPa near the outer cast iron surface. From here they increased into tension to a maximum tensile value of 40 MPa at 4.8 mm before decreasing gradually into compression to reach -9 MPa at 24.0 mm deep. The 'hoop' residual stresses then fluctuated around this level finishing at 3 MPa at the cast iron/steel tube interface at 46.8 mm deep.

The resolved shear stresses only fluctuated slightly throughout the cast iron, with an average value of 0 MPa and a standard deviation of 2 MPa.

General DHD Comments:

From previous calibration studies, the overall accuracy of the DHD residual stress measurement technique is ±30 MPa (2) assuming isotropic material properties and the presence of residual stresses that remain below 60% of the materials' yield strength. However, this general accuracy cannot be applied to the measured residual stresses at depths within 1 mm of a free surface. At these depths surface edge effects occur (3), and the accuracy of the air gauging equipment and hence measured residual stresses are unknown. Therefore, the measured residual stresses over these depths have been omitted from the tabular and graphical results to avoid confusion.

Bonner (5) studied the effect of stress gradients acting across a Ø 20 mm core and the resulting distortions of a coaxial Ø 3.2 mm reference hole. Bonner found that the measured distortions of the reference hole were due to the relaxation of residual stresses across the entire cross-sectional area of the extracted core. However, Bonner also found that the distortions of the reference hole were approximately eight times more sensitive to the stresses acting at the centre-line of the reference hole than to those acting near the outer diameter of the core.

6 CONCLUSIONS

A single, cast iron insert specimen containing 12 steel tubes was supplied by POSIVA for measurement. Bi-axial residual stress profiles were measured using the DHD technique along 5 measurement lines prescribed by POSIVA. A sixth measurement was also made (mistakenly) and has been presented for interest's sake, but was not part of the contracted work scope. As the specimen was manufactured by casting iron in a cylinder around 12 steel tubes, there was no bond between the two materials. As such, the iron and steel materials have been measured and analysed in separate stages. In measurements 1, 2 and 3 the measurement lines were radially inwards allowing the measurement of true hoop and axial residual stresses. Measurements 4 and 5 were not drilled radially inwards and gave the axial residual stresses as well as a combination of the hoop and radial stress directions, which were referred to as 'hoop' stresses.

An overall nominal accuracy of approximately ±30 MPa is valid for the DHD residual stress measurements at all depths, except at those within 1 mm of the specimen surface. Based on this error bound, many of the 'features' in the residual stress profiles were considered to be measurement fluctuations and were not necessarily due to a changing stress field, but more likely a result of the errors and inaccuracies of the measurement technique.

The measured stress profiles from the 5 prescribed locations showed similar results where the locations are comparable. The axial and hoop residual stresses were shown to be very similar at all locations within the cast iron, but differed in the steel tube sections. In all measurements made from the outer cast iron surface, except for measurement 1, the results showed compressive peaks in the surface regions. The maximum compressive residual stresses in both the axial and hoop directions were -113 MPa and -81 MPa respectively, both found at the surface of measurement 3. Generally the compressive peaks were followed by sharp rises into tension by both the axial and hoop stresses. Once in tension the results showed tensile peaks occurring in most measurements before 20 mm deep. The maximum tensile stress levels in the cast iron for both the axial and hoop directions were 58 MPa and 57 MPa respectively, both found at approximately 2 mm from the surface of measurement 1. The exception to this was measurement 3 in which peaks, particularly in the hoop direction, occurred at the specimen centre and at approximately 170 mm deep, where the measurement was not adjacent to a steel tube wall. This was confirmed by measurement 5, which was made across the region between the inner and outer steel tubes, and showed higher 'hoop' stresses.

At all locations the steel tube inserts showed the axial stresses to be higher than hoop or 'hoop' stresses. A maximum axial residual stress value in the steel tubing of 118 MPa was recorded near the cast iron/steel tube interface of measurement 1, whilst a minimum axial stress value of 15 MPa was seen at the inner surface of the steel tube in measurement 2. The maximum hoop residual stress was 64 MPa recorded towards the inner surface of the steel tube in measurement 1 with the most compressive hoop value of -61 MPa recorded at the cast iron/steel tube interface in measurement 2.

To finally conclude, other than at the surface of the cast iron and in the steel tubes, there were very few discernable or significant residual stresses in the bulk of the cast iron. The highest tensile stresses in the bulk cast iron were shown to be at the surface of measurement 1 and in the central regions not adjacent to the steel tube walls.

7 REFERENCES

[1]. **Contract Documentation.**

- E-mail: Nolvi Leena (POSIVA), *"Residual stress measurements on a cast iron insert"*, 21/03/2011.
- Quotation: Ed Kingston (VEQTER Ltd), Q11-001, 04/04/2011.
- Purchase Order: POSIVA, 9388-11, 24/5/2011.
- E-mail: Ed Kingston (VEQTER Ltd), *"RE: Residual stress measurements on a cast iron insert / schedule for testing"*, 28/06/2011.
- E-mail: Nolvi Leena (POSIVA), *"Visit"*, 07/07/2011.
- E-mail: Nolvi Leena (POSIVA), *"VS: Visit"*, 07/07/2011.

[2]. **George, D. F. B. et al.** *Measurement of Through-Thickness Stresses Using Small Holes.* s.l. : Journal of Strain Analysis for Engineering Design, 2002. No. 2 Vol. 7.

[3]. **Garcia Grenada, A. A. et al.** *"Assessment of Distortions in the Deep Hole Technique for Measuring Residual Stresses".* Oxford : Proceedings of the 11th International Conference on Experimental Mechanics, 1998. pp: 1301-1306.

[4]. **Goudar, D. M. et al.** *"Evaluating Uncertainty in residual stress measured using the deep-hole drilling technique".* s.l. : Strain, 2009. Vol. 47 pp: 62-74.

[5]. **Bonner, N. W.** *"Measurement of Residual Stress in Thick-Section Steel Welds".* University of Bristol : PhD Thesis, 1996.

8 TABLES

Table 1: DHD measured residual stress results for the measurement 1 location (reduced data set).

Depth (mm)	Axial Stress (MPa)	Hoop Stress (MPa)	Shear Stress (MPa)	Axial Error (MPa)	Hoop Error (MPa)	Shear Error (MPa)	Young's Modulus (GPa)
0.0-0.8	Omitted due to free surface						N/A
1	10.3	24.7	-8.5	19.7	17.6	9.6	166
2	57.9	56.6	-13.1	16.8	16.8	9.5	166
3	35.8	42.3	-7.0	16.5	16.4	9.6	166
4	25.5	41.7	4.4	16.4	16.4	9.5	166
5	20.4	30.5	11.0	17.6	16.5	9.5	166
6	27.9	25.0	10.0	16.4	17.1	9.5	166
7	31.4	21.2	4.4	18.5	16.8	9.5	166
8	29.3	16.1	-0.4	16.5	16.7	9.6	166
9	18.7	16.0	0.4	16.9	17.6	9.5	166
10	14.5	21.5	0.3	17.6	18.1	9.5	166
11	7.5	17.1	-1.2	16.5	16.5	9.6	166
12	-1.3	9.3	-5.0	17.5	17.9	9.5	166
13	7.3	14.8	-7.9	16.5	16.4	9.8	166
14	8.0	16.3	-0.9	17.8	16.5	9.6	166
15	-4.2	20.3	-0.3	48.5	16.3	16.1	166
16	8.6	22.0	-4.9	18.5	16.7	11.1	166
17	7.5	18.0	-2.8	17.0	16.7	9.5	166
18	7.5	20.2	-4.9	16.4	16.4	9.6	166
19	2.1	16.8	-6.0	16.3	16.4	9.4	166
20	7.3	18.6	-2.2	16.9	16.4	9.3	166
21	6.4	10.1	-0.2	16.6	18.0	9.6	166
22	6.7	-3.0	-5.2	19.5	18.3	9.4	166
23	7.7	3.1	-7.1	16.9	16.5	9.5	166
24	2.9	1.9	-5.8	16.6	16.8	9.4	166
25	6.8	1.3	-8.4	16.4	17.2	9.5	166
26	-1.0	4.1	-9.7	16.4	16.3	9.6	166
27	-7.7	2.6	-10.1	16.4	16.4	9.4	166
28	-5.8	16.4	-9.9	20.4	19.1	9.5	166
29	-0.9	13.0	-8.2	21.2	24.4	9.6	166
30	5.8	6.1	-8.8	16.8	16.7	9.5	166
31	-3.0	-1.4	-7.2	16.9	16.6	9.4	166
32	-13.9	-8.3	-6.0	16.5	16.5	9.4	166
33	-26.3	-17.0	-13.8	16.6	17.6	9.5	166
34	-22.5	-21.5	-10.0	16.3	16.6	9.4	166
35	-19.4	-13.3	-4.1	18.3	18.0	9.5	166
36	-17.4	-11.4	4.8	16.5	16.7	9.5	166
37	-26.4	-36.6	9.2	16.6	17.0	9.8	166
38	Omitted due to free surfaces						166

Depth (mm)	Axial Stress (MPa)	Hoop Stress (MPa)	Shear Stress (MPa)	Axial Error (MPa)	Hoop Error (MPa)	Shear Error (MPa)	Young's Modulus (GPa)
39							166
40	116.9	50.5	-5.6	18.9	18.3	10.7	210
41	113.9	41.9	-7.4	18.2	18.0	10.4	210
42	101.9	26.7	-10.1	18.2	18.0	10.3	210
43	96.8	18.6	-12.3	20.1	19.5	10.4	210
44	103.1	22.8	-11.7	18.9	18.9	10.3	210
45	113.9	46.8	-9.2	19.0	18.9	10.2	210
46	111.9	58.6	-10.5	18.3	17.9	10.2	210
47	111.0	64.0	-9.6	19.6	18.9	10.2	210

Table 2: DHD measured residual stress results for the measurement 2 location (reduced data set).

Depth (mm)	Axial Stress (MPa)	Hoop Stress (MPa)	Shear Stress (MPa)	Axial Error (MPa)	Hoop Error (MPa)	Shear Error (MPa)	Young's Modulus (GPa)
0.0-0.8	Omitted due to free surfaces						N/A
1	-62.0	-41.0	0.0	23.0	28.0	11.2	166
2	-21.0	-6.9	-0.5	20.4	24.8	11.1	166
3	-5.1	4.9	-1.0	20.3	24.9	10.8	166
4	1.5	9.2	-1.8	21.1	24.7	10.5	166
5	3.7	10.5	-2.4	21.3	24.9	10.6	166
6	3.3	10.3	-2.9	21.3	24.7	10.5	166
7	1.8	9.4	-3.2	20.4	24.6	10.5	166
8	0.2	8.6	-3.5	20.7	25.3	10.6	166
9	-1.0	7.9	-3.8	21.1	24.9	10.5	166
10	-1.8	7.2	-4.0	24.6	25.4	10.5	166
11	-2.5	6.3	-3.7	23.7	26.8	10.4	166
12	-2.8	6.7	-3.5	20.3	26.0	10.4	166
13	-2.9	7.9	-3.0	19.3	22.7	10.4	166
14	-3.0	9.6	-2.7	19.8	22.6	10.5	166
15	-2.7	11.8	-2.3	21.9	23.6	10.4	166
16	-2.3	13.8	-1.5	18.8	23.3	10.3	166
17	-1.8	15.4	-0.3	22.9	23.1	10.4	166
18	-1.6	16.6	0.9	21.6	22.9	10.5	166
19	-1.9	16.7	1.9	18.1	21.4	10.6	166
20	-2.5	15.9	2.5	18.1	21.6	10.5	166
21	-2.9	14.2	2.6	18.6	21.8	10.4	166
22	-3.0	11.7	2.5	18.3	21.0	10.5	166
23	-3.2	9.3	2.4	18.0	20.8	10.5	166
24	-3.2	7.8	2.2	18.0	20.8	10.5	166
25	-2.7	7.2	2.0	18.5	20.6	10.4	166
26	-1.7	7.0	2.0	18.3	20.6	10.4	166
27	-0.9	6.9	2.0	18.1	20.7	10.6	166

Depth (mm)	Axial Stress (MPa)	Hoop Stress (MPa)	Shear Stress (MPa)	Axial Error (MPa)	Hoop Error (MPa)	Shear Error (MPa)	Young's Modulus (GPa)
28	0.2	7.4	1.8	18.1	20.8	10.9	166
29	1.2	8.7	1.8	19.3	20.7	10.4	166
30	1.7	9.9	1.6	19.5	21.4	10.3	166
31	1.4	10.4	1.7	18.1	20.3	10.3	166
32	1.3	10.7	2.1	18.0	20.3	10.5	166
33	1.2	10.9	2.6	18.9	20.5	10.5	166
34	1.2	10.8	2.8	20.7	20.8	10.5	166
35	1.5	10.9	2.9	19.4	20.7	10.4	166
36	2.1	11.6	3.1	18.5	20.1	10.4	166
37	2.3	12.3	3.5	19.1	20.3	11.1	166
38	2.1	12.7	3.8	18.4	21.2	10.8	166
39	1.8	13.0	3.8	19.4	19.9	10.6	166
40	1.6	13.1	3.4	20.3	20.3	10.5	166
41	1.2	12.5	2.9	18.1	19.5	10.9	166
42	0.6	11.9	2.4	18.6	20.2	10.4	166
43	0.1	11.4	2.0	19.7	20.5	10.4	166
44	-0.2	11.1	1.6	18.6	20.0	10.4	166
45	-0.4	10.8	1.4	17.8	19.3	10.4	166
46	-0.7	10.5	1.2	18.2	19.5	10.5	166
47	-1.1	10.2	0.9	19.8	20.6	10.4	166
48	-1.5	9.5	0.8	18.2	20.0	10.4	166
49	-2.0	8.8	0.6	17.8	19.1	10.7	166
50	-2.6	7.8	0.5	17.7	19.2	10.4	166
51	-2.8	7.2	0.4	18.0	20.1	10.5	166
52	-2.6	7.1	0.5	19.2	19.9	10.5	166
53	-1.9	7.4	0.6	18.5	19.2	10.7	166
54	-1.0	7.8	0.8	18.2	19.4	10.3	166
55	-0.3	8.2	1.0	17.9	19.2	10.3	166
56	0.1	8.6	1.3	17.7	18.7	10.3	166
57	0.0	8.8	1.7	18.0	19.1	10.3	166
58	-0.2	9.1	2.0	18.0	18.9	10.3	166
59	-0.8	9.2	2.2	19.1	19.2	10.3	166
60	-2.3	8.3	2.4	20.3	20.4	10.3	166
61	-4.2	6.9	2.5	18.9	18.5	10.5	166
62	-6.8	4.8	2.4	18.0	18.7	10.4	166
63	-9.0	2.5	2.2	20.4	19.6	10.3	166
64	-10.5	0.6	1.8	18.6	19.5	10.4	166
65	-11.1	-0.6	1.6	17.6	18.5	10.3	166
66	-11.0	-0.5	1.4	17.6	18.4	10.3	166
67	-10.2	0.3	1.2	17.7	18.4	10.2	166
68	-8.4	1.5	1.0	17.6	18.6	10.3	166
69	-6.8	2.2	1.0	18.9	18.6	10.3	166
70	-6.1	2.8	1.3	19.5	19.0	10.5	166

Depth (mm)	Axial Stress (MPa)	Hoop Stress (MPa)	Shear Stress (MPa)	Axial Error (MPa)	Hoop Error (MPa)	Shear Error (MPa)	Young's Modulus (GPa)
71	-6.1	2.6	1.4	18.4	19.0	10.3	166
72	-6.5	1.9	1.3	18.3	18.8	10.2	166
73	-7.5	1.3	1.1	17.6	18.2	10.2	166
74	-9.0	0.6	1.0	17.8	18.5	10.3	166
75	-10.5	0.6	1.1	19.5	19.2	10.3	166
76	-11.8	1.5	1.2	20.6	19.3	10.5	166
77	-12.3	2.6	1.3	19.0	18.9	10.4	166
78	-11.4	3.5	1.3	20.3	20.4	10.4	166
79	-10.6	3.1	1.2	24.4	19.1	11.7	166
80	-10.4	2.1	1.1	19.4	18.1	10.6	166
81	-11.2	0.6	0.8	19.1	18.1	10.4	166
82	-12.2	-0.6	0.6	17.8	18.1	10.3	166
83	-12.6	-1.2	0.4	18.4	18.1	10.4	166
84	-12.6	-0.7	0.4	18.4	18.4	10.3	166
85	-12.6	-0.3	0.5	18.6	19.1	10.3	166
86	-12.6	-0.1	0.4	19.4	19.0	10.3	166
87	-12.6	-0.3	0.4	17.9	18.1	10.3	166
88	-12.7	-0.8	0.4	19.7	18.5	10.3	166
89	-12.6	-1.1	0.4	21.7	20.6	10.3	166
90	-12.7	-1.3	0.5	21.8	21.1	10.4	166
91	-13.0	-1.3	0.8	19.4	18.6	10.4	166
92	-13.0	-0.6	0.7	18.0	18.2	10.4	166
93	-12.6	0.5	0.4	17.9	18.2	10.6	166
94	-11.6	2.4	0.0	18.0	18.2	10.4	166
95	-9.7	4.9	-0.6	18.6	18.9	10.4	166
96	-7.3	7.3	-1.3	18.7	20.4	10.4	166
97	-5.1	8.8	-2.0	22.9	23.6	10.5	166
98	-3.3	9.1	-2.5	27.1	27.4	10.4	166
99	-2.6	8.9	-2.6	23.1	26.9	10.4	166
100	-2.9	8.2	-2.3	19.7	19.7	10.4	166
101	-3.9	6.9	-1.8	17.7	17.9	10.3	166
102	-5.1	5.5	-1.1	17.7	17.9	10.3	166
103	-6.3	4.1	-0.5	21.3	19.4	10.3	166
104	-7.5	2.9	-0.1	21.1	18.5	10.3	166
105	-8.6	1.8	0.0	20.8	18.7	10.3	166
106	-9.3	0.9	0.1	19.5	19.4	10.3	166
107	-9.8	0.4	0.0	18.4	18.1	10.3	166
108	-9.8	0.3	-0.1	17.9	18.6	10.3	166
109	-9.6	0.5	0.0	18.1	18.6	10.3	166
110	-9.4	0.4	0.0	18.6	19.7	10.3	166
111	-9.1	0.4	0.0	18.0	17.8	10.3	166
112	-8.8	0.4	0.0	17.8	17.7	10.3	166
113	-8.7	0.4	-0.1	18.3	18.0	10.3	166

Depth (mm)	Axial Stress (MPa)	Hoop Stress (MPa)	Shear Stress (MPa)	Axial Error (MPa)	Hoop Error (MPa)	Shear Error (MPa)	Young's Modulus (GPa)
114	-8.6	0.6	-0.2	17.9	17.8	10.3	166
115	-8.5	1.1	-0.3	18.1	17.7	10.3	166
116	-8.0	1.9	-0.3	18.6	19.0	10.3	166
117	-7.3	3.0	-0.3	18.5	18.1	10.3	166
118	-6.5	4.3	-0.4	18.2	18.7	10.5	166
119	-6.2	5.4	-0.4	17.7	17.7	10.3	166
120	-6.4	5.8	-0.2	19.6	18.3	10.2	166
121	-7.1	5.6	0.0	19.9	19.4	10.3	166
122	-7.7	5.3	0.3	18.2	19.4	10.3	166
123	-7.4	5.2	0.6	19.5	19.8	10.5	166
124	-6.3	5.5	0.7	18.1	18.5	10.3	166
125	-5.4	5.4	0.6	17.9	17.8	10.3	166
126	-5.3	4.7	0.4	17.9	18.4	10.3	166
127	-6.0	3.6	0.1	18.1	18.7	10.4	166
128	-6.9	2.7	-0.2	18.5	18.0	10.3	166
129	-7.6	2.6	-0.4	18.0	17.9	10.3	166
130	-7.8	3.2	-0.6	19.0	19.3	10.3	166
131	-7.7	3.9	-0.7	18.5	19.2	10.3	166
132	-7.8	4.8	-0.8	18.4	18.3	10.3	166
133	-7.6	5.8	-0.8	20.2	19.2	10.4	166
134	-7.4	6.8	-0.9	18.9	18.3	10.2	166
135	-7.0	7.7	-1.0	19.7	20.2	10.2	166
136	-6.2	8.3	-1.2	20.4	18.8	10.2	166
137	-5.5	8.9	-1.6	18.1	17.8	10.2	166
138	-4.6	9.2	-1.9	18.2	18.0	10.2	166
139	-3.7	9.7	-2.2	22.8	21.4	10.2	166
140	-2.7	10.1	-2.6	19.8	19.3	10.2	166
141	-1.9	10.6	-2.8	19.2	18.4	10.3	166
142	-1.2	11.1	-3.0	18.0	17.8	10.2	166
143	-0.6	11.6	-3.0	18.0	17.9	10.2	166
144	-0.2	12.2	-2.9	18.2	17.8	10.2	166
145	0.2	12.6	-2.7	22.8	24.1	10.3	166
146	0.7	12.9	-2.7	21.4	23.3	10.2	166
147	1.0	13.0	-2.7	22.7	26.3	10.4	166
148	1.3	13.2	-2.5	24.5	25.8	10.7	166
149	1.4	13.3	-2.4	18.1	18.0	10.3	166
150	1.6	13.5	-2.3	18.1	18.0	10.4	166
151	1.9	13.7	-2.2	19.8	20.5	10.3	166
152	2.0	13.7	-1.9	23.0	22.7	10.4	166
153	2.3	13.8	-1.7	18.8	18.1	10.5	166
154	2.4	13.9	-1.5	24.4	22.5	10.2	166
155	2.7	14.1	-1.4	22.7	24.7	10.3	166
156	2.8	14.3	-1.4	18.7	18.7	10.6	166

Depth (mm)	Axial Stress (MPa)	Hoop Stress (MPa)	Shear Stress (MPa)	Axial Error (MPa)	Hoop Error (MPa)	Shear Error (MPa)	Young's Modulus (GPa)
157	2.8	14.4	-1.4	19.6	20.4	10.3	166
158	2.8	14.5	-1.4	19.3	19.0	10.4	166
159	2.7	14.5	-1.5	19.2	18.7	10.4	166
160	2.5	14.4	-1.5	19.6	19.1	10.4	166
161	2.4	14.5	-1.5	23.4	22.3	10.4	166
162	2.5	14.7	-1.5	33.4	34.6	10.3	166
163	2.5	14.8	-1.4	36.0	39.4	10.3	166
164	2.6	14.7	-1.3	26.7	23.9	10.2	166
165	2.8	14.7	-1.2	18.6	19.0	10.3	166
166	3.0	14.8	-1.2	18.3	18.3	10.2	166
167	3.1	14.9	-1.2	23.1	22.5	10.2	166
168	3.3	15.0	-1.1	45.0	45.1	10.3	166
169	3.3	15.1	-1.1	50.4	51.6	10.3	166
170	3.2	15.3	-1.2	27.8	23.7	10.3	166
171	3.2	15.6	-1.2	18.8	19.1	10.3	166
172	3.0	15.7	-1.1	18.4	18.4	10.3	166
173	2.9	15.7	-1.0	19.2	18.6	10.3	166
174	2.6	15.6	-1.0	19.0	18.6	10.5	166
175	2.2	15.3	-0.8	18.6	19.0	10.3	166
176	1.8	14.9	-0.8	19.9	20.7	10.4	166
177	1.4	14.3	-0.8	18.9	20.3	10.5	166
178	0.9	13.7	-0.8	22.2	25.7	10.3	166
179	0.4	13.3	-0.9	18.5	18.8	10.4	166
180	0.1	13.1	-1.2	19.9	20.2	10.3	166
181	0.0	13.0	-1.5	19.3	19.6	10.4	166
182	-0.1	12.5	-1.9	18.2	18.6	10.5	166
183	-0.3	11.7	-2.4	18.5	18.2	10.4	166
184	-0.8	11.1	-2.8	18.3	18.2	10.4	166
185	-1.2	10.4	-2.9	18.8	18.8	10.3	166
186	-1.9	9.5	-3.0	19.2	19.1	10.3	166
187	-2.5	9.0	-2.9	18.9	18.6	10.3	166
188	-3.0	8.8	-2.8	18.8	18.5	10.3	166
189	-3.5	8.5	-2.6	18.2	18.5	10.3	166
190	-3.9	8.3	-2.5	18.6	18.2	10.3	166
191	-4.7	8.1	-2.4	18.0	18.2	10.4	166
192	-6.0	7.8	-2.4	18.0	18.1	10.4	166
193	-7.4	7.2	-2.4	18.5	18.4	10.4	166
194	-8.8	6.9	-2.3	19.1	19.4	10.5	166
195	-9.7	7.1	-2.2	18.1	18.4	10.5	166
196	-9.9	7.8	-2.1	18.0	18.1	10.5	166
197	-9.8	8.6	-2.0	18.4	18.0	10.3	166
198	-9.5	9.2	-1.8	26.3	25.1	10.4	166
199	-9.1	9.8	-1.7	25.2	26.8	10.5	166

Depth (mm)	Axial Stress (MPa)	Hoop Stress (MPa)	Shear Stress (MPa)	Axial Error (MPa)	Hoop Error (MPa)	Shear Error (MPa)	Young's Modulus (GPa)
200	-8.8	10.3	-1.6	19.9	21.0	10.4	166
201	-8.7	10.3	-1.4	23.5	23.4	10.4	166
202	-8.5	10.4	-1.3	17.8	17.9	10.4	166
203	-8.2	10.8	-1.3	18.1	18.1	10.4	166
204	-8.1	11.0	-1.3	18.7	18.7	10.4	166
205	-8.1	11.0	-1.4	19.1	18.3	10.4	166
206	-8.0	10.7	-1.8	19.6	19.0	10.4	166
207	-8.0	10.2	-2.1	19.3	19.3	10.4	166
208	-8.2	9.1	-2.6	18.2	18.0	10.6	166
209	-7.9	7.9	-3.1	17.8	18.0	10.4	166
210	-7.2	6.5	-3.2	17.9	18.0	10.4	166
211	-6.3	5.0	-3.2	17.9	18.1	10.4	166
212	-5.4	3.1	-3.0	18.0	18.0	10.4	166
213	Omitted due to free surfaces						N/A
214							N/A
215	41.4	-53.0	8.6	19.0	19.3	10.4	210
216	55.7	-32.1	4.1	19.6	20.0	10.4	210
217	65.0	-18.6	0.9	19.0	18.0	10.8	210
218	69.4	-4.7	1.9	18.7	18.4	10.6	210
219	72.1	10.1	2.2	18.0	18.3	10.7	210
220	66.9	15.5	3.1	18.1	17.9	10.5	210
221	51.4	12.4	3.4	18.0	17.9	10.6	210
222	24.6	0.5	4.2	18.1	18.1	10.5	210

Table 3: DHD measured residual stress results for the measurement 3 location (reduced data set).

Depth (mm)	Axial Stress (MPa)	Hoop Stress (MPa)	Shear Stress (MPa)	Axial Error (MPa)	Hoop Error (MPa)	Shear Error (MPa)	Young's Modulus (GPa)
0.0-0.8	Omitted due to free surface						N/A
1	-112.8	-80.8	-1.9	11.6	10.4	6.4	166
2	-95.6	-79.3	-0.6	12.9	13.5	5.9	166
3	-78.5	-67.8	0.3	10.8	10.3	5.8	166
4	-66.0	-58.5	0.5	10.5	10.3	5.9	166
5	-57.1	-51.7	0.5	10.3	10.2	5.8	166
6	-50.3	-46.3	-0.4	10.4	10.4	5.8	166
7	-45.4	-41.6	-1.3	10.2	10.2	5.9	166
8	-41.8	-37.2	-2.3	10.4	10.2	6.0	166
9	-39.1	-33.0	-3.1	10.3	10.2	5.8	166
10	-37.3	-29.8	-3.5	10.6	11.0	6.1	166
11	-36.1	-27.7	-3.6	11.7	12.0	5.9	166
12	-33.8	-24.4	-3.6	10.6	10.3	5.9	166
13	-30.7	-20.1	-3.6	10.2	10.3	5.9	166

Depth (mm)	Axial Stress (MPa)	Hoop Stress (MPa)	Shear Stress (MPa)	Axial Error (MPa)	Hoop Error (MPa)	Shear Error (MPa)	Young's Modulus (GPa)
14	-27.7	-15.8	-4.0	10.6	10.4	6.0	166
15	-24.3	-11.7	-4.4	10.2	10.2	5.9	166
16	-21.2	-8.5	-4.8	10.3	10.2	5.9	166
17	-18.4	-6.3	-5.3	10.7	10.3	5.9	166
18	-16.4	-4.7	-5.3	10.6	10.4	5.9	166
19	-15.0	-3.1	-5.5	10.2	10.2	6.0	166
20	-14.1	-1.7	-5.9	10.7	10.6	6.0	166
21	-13.1	-0.7	-5.8	10.3	10.3	5.9	166
22	-12.7	-0.1	-5.9	10.6	10.8	5.9	166
23	-12.9	-0.6	-5.9	11.3	11.2	6.0	166
24	-12.9	-0.5	-5.8	10.8	10.6	6.0	166
25	-13.2	-0.7	-5.5	10.4	10.3	5.9	166
26	-13.3	-0.8	-5.6	11.3	11.2	5.9	166
27	-12.8	-0.1	-5.8	10.7	10.7	6.1	166
28	-12.8	0.0	-5.7	10.2	10.3	6.0	166
29	-13.3	-0.1	-5.5	10.7	10.3	5.9	166
30	-13.5	-0.1	-5.3	10.9	10.2	6.1	166
31	-13.5	-0.1	-5.4	10.4	10.2	6.1	166
32	-13.6	-0.2	-5.6	10.3	10.3	6.2	166
33	-13.9	-0.5	-5.3	12.3	11.3	6.3	166
34	-15.7	-1.3	-4.3	12.3	12.1	6.1	166
35	-16.9	-1.1	-3.4	10.3	10.3	5.9	166
36	-15.8	-0.1	-3.3	10.5	10.5	6.0	166
37	-14.3	0.4	-3.5	11.6	11.4	6.0	166
38	-13.2	0.7	-3.7	11.1	11.0	5.9	166
39	-13.0	0.8	-4.2	10.4	10.8	6.0	166
40	-13.3	0.5	-4.3	10.2	10.4	5.9	166
41	-13.5	0.4	-4.4	10.4	10.2	5.9	166
42	-13.6	0.5	-4.4	10.9	10.8	5.9	166
43	-14.2	0.1	-4.3	10.8	10.5	5.9	166
44	-14.2	0.2	-4.4	10.5	10.4	6.0	166
45	-13.6	0.5	-4.9	10.6	10.4	5.9	166
46	-13.2	0.6	-5.0	10.3	10.3	6.0	166
47	-12.8	0.7	-5.1	10.3	10.4	5.9	166
48	-12.4	0.9	-5.3	10.3	10.3	6.0	166
49	-12.1	1.3	-5.3	10.3	10.3	6.1	166
50	-12.0	1.6	-5.3	10.3	10.2	5.9	166
51	-12.2	1.7	-5.2	10.2	10.2	5.9	166
52	-12.4	1.4	-5.3	10.4	10.3	5.9	166
53	-12.7	1.0	-5.5	11.0	10.9	5.9	166
54	-13.1	0.9	-5.3	10.3	10.5	5.9	166
55	-13.5	0.8	-5.0	10.6	10.8	6.0	166
56	-14.0	0.7	-4.9	10.5	10.9	6.0	166

Depth (mm)	Axial Stress (MPa)	Hoop Stress (MPa)	Shear Stress (MPa)	Axial Error (MPa)	Hoop Error (MPa)	Shear Error (MPa)	Young's Modulus (GPa)
57	-14.7	0.8	-4.6	10.4	10.6	6.1	166
58	-15.3	0.4	-4.2	10.3	10.2	6.0	166
59	-15.4	0.4	-4.0	10.2	10.3	6.0	166
60	-15.0	1.0	-4.1	10.2	10.3	5.9	166
61	-14.1	1.6	-4.6	10.2	10.3	5.9	166
62	-13.4	2.3	-4.8	10.2	10.4	6.0	166
63	-13.6	2.6	-4.6	10.3	10.2	5.9	166
64	-13.2	3.2	-4.7	10.3	10.3	5.9	166
65	-12.6	3.9	-4.9	10.2	10.3	5.9	166
66	-11.7	4.7	-5.6	10.4	10.3	6.0	166
67	-10.6	5.5	-6.1	10.2	10.3	5.9	166
68	-10.7	6.0	-6.0	10.3	10.3	5.9	166
69	-11.3	6.8	-5.6	10.3	10.4	5.9	166
70	-11.2	8.0	-5.6	10.6	10.9	5.9	166
71	-11.1	8.6	-5.8	10.3	10.4	5.9	166
72	-11.8	8.5	-5.7	10.3	10.2	5.9	166
73	-12.5	8.0	-5.4	10.5	10.7	5.9	166
74	-12.9	7.4	-5.4	10.4	10.5	5.9	166
75	-12.7	7.0	-5.6	10.2	10.3	5.9	166
76	-12.1	6.9	-6.2	10.4	10.4	5.9	166
77	-12.1	6.4	-6.7	10.4	10.6	6.1	166
78	-12.2	6.1	-7.1	10.4	10.5	5.9	166
79	-12.7	5.6	-7.4	10.3	10.3	5.9	166
80	-13.2	5.0	-7.8	10.2	10.2	6.0	166
81	-13.6	4.5	-7.8	10.3	10.4	5.9	166
82	-14.5	4.0	-7.8	10.4	10.6	5.9	166
83	-14.6	4.1	-7.9	10.6	10.5	5.9	166
84	-14.9	4.1	-7.7	10.2	10.3	5.9	166
85	-15.1	4.0	-7.2	10.2	10.2	5.9	166
86	-15.3	3.7	-6.4	10.3	10.2	5.9	166
87	-15.5	3.3	-5.6	10.4	10.3	5.9	166
88	-15.6	3.0	-4.8	10.3	10.3	5.9	166
89	-15.4	2.8	-4.1	10.3	10.2	5.9	166
90	-15.3	2.8	-3.3	10.3	10.3	5.9	166
91	-15.0	3.1	-2.8	10.3	10.2	5.9	166
92	-14.6	3.5	-2.5	10.2	10.3	5.9	166
93	-14.1	3.7	-2.4	10.4	10.3	6.0	166
94	-13.5	4.1	-2.5	10.2	10.2	5.9	166
95	-12.9	4.4	-2.5	10.4	10.5	5.9	166
96	-12.4	4.7	-2.6	10.4	10.3	6.0	166
97	-12.1	5.1	-3.2	10.3	10.5	5.9	166
98	-11.3	5.5	-3.6	10.4	10.5	5.9	166
99	-9.5	6.4	-3.8	10.2	10.2	5.9	166

Depth (mm)	Axial Stress (MPa)	Hoop Stress (MPa)	Shear Stress (MPa)	Axial Error (MPa)	Hoop Error (MPa)	Shear Error (MPa)	Young's Modulus (GPa)
100	-6.5	7.4	-4.2	10.3	10.2	5.9	166
101	-2.8	8.8	-5.1	10.2	10.3	5.9	166
102	-0.4	9.9	-5.6	10.2	10.2	5.9	166
103	1.4	10.6	-5.9	10.3	10.2	5.9	166
104	2.8	11.0	-6.0	10.7	10.5	5.9	166
105	3.9	11.1	-5.9	10.3	10.2	6.0	166
106	4.6	10.8	-5.6	10.2	10.2	6.1	166
107	5.1	10.8	-5.3	10.3	10.2	5.9	166
108	5.8	11.0	-5.0	10.2	10.4	5.9	166
109	6.3	11.1	-4.6	10.2	10.4	5.9	166
110	6.3	11.0	-4.2	10.3	10.3	5.9	166
111	6.6	11.5	-4.1	10.2	10.3	5.9	166
112	6.4	11.4	-3.7	10.2	10.2	5.9	166
113	5.3	10.6	-2.9	10.2	10.2	5.9	166
114	3.8	10.0	-2.4	10.4	10.6	6.1	166
115	2.7	9.1	-2.2	10.2	10.2	5.9	166
116	1.7	8.5	-2.0	10.3	10.2	5.9	166
117	1.0	8.9	-1.8	10.2	10.4	5.9	166
118	0.6	9.2	-1.8	10.6	10.4	5.9	166
119	0.3	9.4	-2.2	10.3	10.2	5.9	166
120	0.6	9.8	-2.7	10.2	10.5	5.9	166
121	1.2	10.0	-3.2	10.3	10.7	5.9	166
122	2.4	10.5	-3.6	11.4	11.8	6.1	166
123	3.6	11.4	-3.9	10.6	11.3	6.0	166
124	4.6	12.3	-4.4	10.3	10.2	5.9	166
125	5.1	13.1	-4.9	10.5	10.3	6.0	166
126	5.5	13.5	-5.7	10.2	10.3	5.9	166
127	6.0	13.9	-6.5	10.3	10.6	5.9	166
128	6.2	14.1	-6.9	10.3	10.2	5.9	166
129	6.0	14.0	-6.9	10.3	10.2	5.9	166
130	5.3	13.3	-6.6	10.3	10.3	5.9	166
131	4.3	12.5	-6.4	10.8	10.5	5.9	166
132	3.7	12.2	-6.4	10.2	10.2	5.9	166
133	3.0	11.6	-6.4	10.3	10.2	5.9	166
134	2.5	10.8	-5.9	10.4	10.5	6.0	166
135	1.7	9.6	-5.3	10.2	10.2	5.9	166
136	1.1	7.8	-4.9	10.3	10.3	5.9	166
137	0.2	5.5	-4.3	10.2	10.4	5.9	166
138	0.1	5.0	-4.3	10.3	10.2	5.9	166
139	0.3	5.1	-4.3	10.2	10.2	5.9	166
140	0.7	5.4	-4.4	10.3	10.4	5.9	166
141	0.6	5.4	-4.2	10.7	10.7	5.9	166
142	0.5	6.0	-4.1	10.5	10.4	5.9	166

Depth (mm)	Axial Stress (MPa)	Hoop Stress (MPa)	Shear Stress (MPa)	Axial Error (MPa)	Hoop Error (MPa)	Shear Error (MPa)	Young's Modulus (GPa)
143	0.3	6.3	-4.0	10.2	10.5	6.0	166
144	0.2	6.1	-4.0	10.5	10.4	5.9	166
145	0.7	6.0	-4.3	10.2	10.2	6.0	166
146	0.6	5.4	-4.2	10.6	10.4	5.9	166
147	0.0	5.4	-4.3	10.8	10.8	5.9	166
148	-0.5	5.8	-4.3	10.4	10.5	6.1	166
149	-0.8	6.1	-4.2	10.2	10.2	5.9	166
150	-0.6	6.6	-4.4	10.3	10.4	5.9	166
151	-0.3	6.8	-4.3	10.5	10.3	5.9	166
152	0.0	6.8	-4.1	10.3	10.4	5.9	166
153	-0.1	6.6	-3.9	10.3	10.2	6.0	166
154	-0.6	6.1	-3.7	10.3	10.3	5.9	166
155	-1.3	5.0	-3.2	10.3	10.2	5.9	166
156	-2.0	4.4	-3.2	10.3	10.3	5.9	166
157	-2.3	4.7	-3.5	10.3	10.3	5.9	166
158	-3.0	5.2	-3.7	10.3	10.2	5.9	166
159	-4.0	5.6	-3.7	10.3	10.3	6.0	166
160	-4.9	5.8	-3.8	10.3	10.3	5.9	166
161	-5.6	6.1	-3.9	10.4	10.5	6.0	166
162	-6.2	6.1	-3.7	10.9	11.3	6.4	166
163	-6.7	6.4	-3.5	10.2	10.5	5.9	166
164	-7.7	6.0	-2.5	10.2	10.2	5.9	166
165	-8.5	5.4	-0.8	10.3	10.3	6.0	166
166	-9.3	4.6	0.9	10.2	10.2	5.9	166
167	-9.9	3.8	1.9	10.3	10.2	5.9	166
168	-10.2	3.2	2.5	10.2	10.4	5.9	166
169	-10.5	3.0	2.8	10.2	10.2	5.9	166
170	-10.3	3.4	2.7	10.3	10.3	5.9	166
171	-10.1	3.6	2.5	10.3	10.4	6.0	166
172	-10.5	3.5	2.4	10.2	10.2	6.0	166
173	-11.1	3.0	2.5	10.2	10.2	5.9	166
174	-11.6	2.7	2.2	10.2	10.2	6.0	166
175	-11.4	2.9	1.5	10.3	10.2	5.9	166
176	-10.9	3.4	0.8	10.3	10.3	5.9	166
177	-10.4	4.0	0.3	10.4	10.5	5.9	166
178	-9.8	4.7	-0.3	10.3	10.2	5.9	166
179	-9.1	5.5	-1.0	10.3	10.3	5.9	166
180	-8.3	6.1	-1.6	10.2	10.2	5.9	166
181	-7.2	6.8	-2.1	10.3	10.3	5.9	166
182	-6.5	7.0	-2.4	10.3	10.3	5.9	166
183	-6.0	7.1	-2.5	10.3	10.2	5.9	166
184	-5.8	7.1	-2.9	10.3	10.2	5.9	166
185	-5.6	7.0	-3.0	10.4	10.3	6.0	166

Depth (mm)	Axial Stress (MPa)	Hoop Stress (MPa)	Shear Stress (MPa)	Axial Error (MPa)	Hoop Error (MPa)	Shear Error (MPa)	Young's Modulus (GPa)
186	-5.6	6.6	-3.0	10.3	10.2	5.9	166
187	-6.2	5.2	-2.5	10.3	10.2	6.0	166
188	-7.2	3.2	-1.6	10.2	10.5	6.0	166
189	-7.8	1.5	-0.8	10.2	10.3	6.0	166
190	-7.5	0.0	-0.7	10.2	10.6	6.1	166
191	-6.6	-0.6	-0.9	10.3	10.2	5.9	166
192	-5.4	-0.2	-1.5	10.3	10.3	5.9	166
193	-4.6	0.3	-2.1	10.2	10.2	5.9	166
194	-4.1	0.9	-2.4	10.2	10.2	5.9	166
195	-4.0	1.3	-2.2	10.2	10.2	5.9	166
196	-4.5	1.4	-1.8	10.2	10.2	5.9	166
197	-6.1	1.0	-1.1	10.2	10.3	5.9	166
198	-7.9	0.5	-0.5	10.3	10.2	5.9	166
199	-9.5	-0.1	-0.2	10.2	10.2	5.9	166
200	-11.0	-0.5	0.0	10.2	10.3	5.9	166
201	-12.5	-1.1	0.3	10.3	10.2	5.9	166
202	-13.7	-1.6	0.4	10.2	10.2	5.9	166
203	-14.2	-2.5	0.5	10.3	10.5	5.9	166
204	-14.3	-3.5	0.5	10.8	11.3	6.2	166
205	-14.1	-3.6	0.4	10.9	10.2	5.9	166
206	-13.7	-3.4	-0.2	10.2	10.6	6.1	166
207	-13.8	-3.3	-0.4	10.2	10.2	5.9	166
208	-12.7	-2.3	-1.0	10.3	10.2	5.9	166
209	-10.9	-0.9	-1.9	10.4	10.3	6.0	166
210	-9.0	0.3	-2.6	10.2	10.2	5.9	166
211	-7.2	1.5	-3.2	10.2	10.2	5.9	166
212	-5.5	2.7	-3.8	10.2	10.2	5.9	166
213	-4.3	3.5	-3.9	10.2	10.3	5.9	166
214	-3.1	4.3	-3.8	10.2	10.2	5.9	166
215	-2.0	5.1	-3.9	10.4	10.3	5.9	166
216	-1.4	5.1	-3.8	10.2	10.2	5.9	166
217	-0.9	4.8	-3.8	10.2	10.2	5.9	166
218	-0.2	5.0	-4.2	10.2	10.4	6.0	166
219	0.2	5.0	-4.2	10.3	10.3	5.9	166
220	0.5	5.0	-4.0	10.3	10.3	5.9	166
221	0.7	5.0	-4.0	10.2	10.2	5.9	166
222	1.0	5.1	-4.0	10.2	10.3	5.9	166
223	1.0	5.0	-4.0	10.2	10.3	5.9	166
224	0.6	4.8	-3.9	10.2	10.2	5.9	166
225	0.4	4.8	-3.9	10.3	10.3	5.9	166
226	0.4	5.0	-4.1	10.3	10.6	6.0	166
227	0.1	4.8	-4.2	10.3	10.3	5.9	166
228	-0.3	4.4	-4.1	10.3	10.2	5.9	166

Depth (mm)	Axial Stress (MPa)	Hoop Stress (MPa)	Shear Stress (MPa)	Axial Error (MPa)	Hoop Error (MPa)	Shear Error (MPa)	Young's Modulus (GPa)
229	-0.9	4.0	-3.8	10.3	10.2	5.9	166
230	-1.8	3.7	-3.2	10.3	10.4	5.9	166
231	-3.1	3.4	-2.3	10.2	10.2	6.0	166
232	-4.1	3.0	-1.4	10.3	10.2	6.0	166
233	-4.6	2.9	-0.8	10.3	10.2	5.9	166
234	-4.6	2.8	-0.6	10.3	10.2	5.9	166
235	-4.3	2.7	-0.5	10.3	10.2	6.0	166
236	-3.8	2.6	-0.6	10.2	10.3	5.9	166
237	-3.5	2.4	-0.5	10.2	10.2	5.9	166
238	-2.8	2.9	-0.9	10.2	10.2	6.1	166
239	-1.9	3.5	-1.3	10.4	10.2	5.9	166
240	-0.7	4.3	-2.0	10.2	10.2	6.0	166
241	0.3	4.8	-2.6	10.9	10.8	5.9	166
242	1.8	5.0	-2.6	11.1	10.8	5.9	166
243	5.8	6.9	-2.5	14.2	14.6	6.1	166
244	3.3	8.1	-2.3	29.4	29.2	6.0	166
245	0.2	11.3	-2.3	10.2	10.3	5.9	166
246	1.8	13.5	-3.2	10.2	10.3	5.9	166
247	2.7	14.5	-3.4	10.6	10.4	5.9	166
248	3.6	14.9	-3.6	10.4	10.3	6.0	166
249	3.7	15.1	-3.5	10.3	10.6	6.0	166
250	4.1	15.4	-3.1	10.3	10.2	5.9	166
251	5.3	15.9	-2.7	10.2	10.2	6.1	166
252	7.2	16.6	-2.3	10.3	10.3	5.9	166
253	7.9	16.9	-2.0	10.7	10.8	5.9	166
254	8.5	17.3	-1.7	10.3	10.3	5.9	166
255	9.8	17.7	-1.5	10.5	10.2	5.9	166
256	10.5	18.0	-1.2	10.4	10.5	5.9	166
257	11.1	19.0	-1.1	10.2	10.3	5.9	166
258	11.7	19.7	-1.2	10.2	10.2	5.9	166
259	11.9	20.3	-1.0	10.4	10.6	5.9	166
260	11.9	20.6	-0.9	10.4	10.3	5.9	166
261	12.7	21.3	-0.8	12.0	11.9	6.8	166
262	12.9	21.6	-0.8	11.8	11.8	6.9	166
263	13.0	21.9	-0.8	11.8	12.0	6.8	166
264	13.2	22.6	-0.9	11.8	11.8	6.8	166
265	13.2	23.4	-1.0	11.8	11.9	6.8	166
266	12.9	23.9	-1.1	11.9	11.9	6.8	166
267	12.1	24.2	-1.6	11.9	11.8	6.8	166
268	9.9	24.1	-2.8	12.1	12.1	6.8	166
269	7.2	23.6	-4.1	11.8	11.9	6.8	166
270	5.4	23.2	-4.9	12.2	12.0	6.8	166
271	4.5	22.5	-5.1	11.8	11.8	6.8	166

Depth (mm)	Axial Stress (MPa)	Hoop Stress (MPa)	Shear Stress (MPa)	Axial Error (MPa)	Hoop Error (MPa)	Shear Error (MPa)	Young's Modulus (GPa)
272	5.8	22.1	-4.9	11.8	11.8	6.8	166
273	8.1	22.3	-4.1	11.8	11.9	6.8	166
274	10.8	23.4	-2.9	12.0	11.9	6.8	166
275	12.3	24.3	-2.1	11.9	11.9	6.8	166
276	12.8	24.9	-1.9	12.8	13.1	6.8	166
277	13.6	25.3	-2.0	12.0	12.1	6.8	166
278	13.6	25.2	-2.2	11.8	11.9	6.9	166
279	12.5	24.9	-2.2	12.1	11.8	6.8	166
280	12.2	24.8	-1.7	12.3	12.3	6.8	166
281	13.1	24.8	-1.5	11.9	12.0	6.8	166
282	13.4	24.3	-1.7	11.9	11.9	6.8	166
283	13.1	24.0	-2.0	11.8	11.9	6.8	166
284	13.1	24.0	-2.0	11.9	11.8	6.8	166
285	12.6	23.7	-1.6	12.0	11.9	6.8	166
286	12.2	23.6	-1.4	12.4	13.1	6.8	166
287	12.2	23.2	-1.5	12.3	12.0	6.9	166
288	12.1	22.7	-1.4	11.9	11.8	6.8	166
289	12.2	22.3	-1.3	11.8	11.9	6.8	166
290	12.5	21.8	-1.5	11.8	11.9	6.8	166
291	13.0	21.1	-1.6	11.9	12.1	6.8	166
292	13.2	20.1	-1.1	12.0	12.0	6.8	166
293	14.1	19.6	-0.2	11.9	11.9	6.8	166
294	16.1	19.6	0.6	11.8	11.9	6.8	166
295	16.8	19.5	1.1	11.8	11.8	6.9	166
296	16.7	19.2	1.0	11.9	12.0	6.8	166
297	16.7	18.6	0.7	11.9	11.8	6.9	166
298	16.1	18.0	0.8	11.8	11.9	6.8	166
299	16.1	17.6	0.8	11.8	11.9	6.8	166
300	16.4	17.1	0.9	12.0	11.9	6.9	166
301	16.7	16.8	1.0	11.8	11.9	6.8	166
302	17.3	16.5	1.2	12.2	12.0	6.8	166
303	18.0	16.3	1.5	12.2	12.3	6.8	166
304	18.0	15.9	1.8	12.0	12.0	6.8	166
305	18.1	15.7	1.9	12.0	11.9	6.8	166
306	17.6	15.2	1.8	11.8	11.8	6.8	166
307	16.7	14.6	1.5	11.9	11.9	7.0	166
308	16.1	14.2	1.4	11.9	11.9	6.9	166
309	15.5	13.6	1.3	12.1	12.0	6.8	166
310	14.5	12.8	1.2	11.9	11.8	6.8	166
311	13.8	12.3	0.7	11.8	11.9	6.8	166
312	13.1	11.7	0.0	11.8	11.9	6.9	166
313	11.7	11.0	-0.5	12.2	12.2	6.8	166
314	10.4	10.6	-0.6	11.9	11.8	6.8	166

Depth (mm)	Axial Stress (MPa)	Hoop Stress (MPa)	Shear Stress (MPa)	Axial Error (MPa)	Hoop Error (MPa)	Shear Error (MPa)	Young's Modulus (GPa)
315	10.2	10.6	-0.6	11.8	11.9	6.8	166
316	10.8	10.7	-0.4	11.9	11.9	6.9	166
317	11.4	10.6	0.1	11.9	11.9	6.8	166
318	11.6	10.2	0.5	11.9	11.9	6.9	166
319	12.5	10.1	0.7	11.9	12.0	6.8	166
320	12.7	9.9	0.9	12.0	11.9	6.8	166
321	11.9	9.5	1.0	12.2	12.1	6.8	166
322	11.1	9.2	1.1	12.2	12.2	6.8	166
323	11.5	9.3	0.9	11.8	11.9	6.8	166
324	11.9	9.4	0.8	12.0	12.0	6.8	166
325	11.1	9.1	0.9	12.1	12.5	6.9	166
326	10.4	9.1	0.7	11.9	12.2	6.8	166
327	10.1	9.2	0.4	12.1	12.0	7.1	166
328	9.9	9.2	0.3	11.9	12.1	6.8	166
329	9.9	9.2	0.2	12.0	12.1	6.8	166
330	9.9	9.2	0.1	11.9	12.0	6.8	166
331	9.4	8.8	0.0	11.8	11.8	6.8	166
332	9.2	8.7	-0.3	11.8	11.9	6.8	166
333	8.9	8.7	-0.6	11.8	11.8	6.8	166
334	8.7	8.7	-0.7	11.8	11.9	6.8	166
335	8.9	8.9	-0.6	11.9	11.8	6.8	166
336	8.9	9.0	-0.4	11.9	11.9	6.8	166
337	8.9	9.0	-0.3	11.9	12.0	6.8	166
338	9.0	9.0	-0.2	12.0	12.0	6.8	166
339	9.2	9.1	-0.1	11.8	11.9	6.8	166
340	9.3	9.2	0.0	12.4	12.5	6.9	166
341	9.5	9.4	0.4	12.1	12.1	6.8	166
342	10.9	9.9	0.6	11.8	11.9	6.8	166
343	12.8	10.5	1.0	11.9	11.8	6.8	166
344	15.0	10.9	1.5	12.0	11.9	6.8	166
345	16.7	11.0	2.1	12.0	11.9	6.9	166
346	17.7	10.8	2.2	12.1	12.1	6.8	166
347	18.0	10.6	2.3	11.8	11.8	6.9	166
348	17.8	10.6	2.3	12.0	12.0	6.8	166
349	18.2	10.7	2.4	11.9	11.9	6.8	166
350	18.9	11.0	3.1	12.6	12.3	6.8	166
351	19.5	11.1	3.3	12.1	12.2	6.9	166
352	19.1	11.1	3.2	11.8	11.8	6.8	166
353	18.1	10.9	3.1	12.1	11.9	6.9	166
354	16.5	10.7	2.7	11.8	11.8	6.9	166
355	14.5	10.2	2.0	12.0	12.0	6.8	166
356	13.9	10.0	1.6	11.9	12.1	6.9	166
357	14.1	9.9	1.5	11.8	11.8	6.8	166

Depth (mm)	Axial Stress (MPa)	Hoop Stress (MPa)	Shear Stress (MPa)	Axial Error (MPa)	Hoop Error (MPa)	Shear Error (MPa)	Young's Modulus (GPa)
358	14.2	9.7	1.5	11.9	12.0	6.8	166
359	14.2	9.6	1.5	11.8	11.8	6.8	166
360	14.7	9.6	1.3	13.4	13.6	7.0	166
361	14.6	9.5	1.6	13.2	12.4	6.8	166
362	14.6	9.5	1.6	12.3	12.0	6.8	166
363	15.2	9.7	1.9	12.0	11.8	6.8	166
364	15.8	9.7	2.1	11.9	12.0	6.9	166
365	16.2	9.6	1.9	11.8	11.9	6.9	166
366	16.4	9.9	1.8	12.0	12.0	6.8	166
367	16.6	10.2	1.7	12.1	11.9	6.8	166
368	16.3	10.5	1.6	12.8	12.4	6.8	166
369	15.1	10.2	1.5	11.9	12.0	6.8	166
370	13.8	9.7	0.9	12.8	12.7	6.9	166
371	12.9	9.1	0.0	11.8	11.9	6.8	166
372	11.8	8.4	-0.3	11.9	11.9	6.9	166
373	11.7	8.1	-0.5	12.0	11.9	6.9	166
374	12.8	8.0	-0.4	11.8	11.8	6.8	166
375	15.0	8.5	0.0	12.1	12.0	6.9	166
376	16.8	9.0	0.5	12.3	11.9	7.0	166
377	16.8	9.4	1.0	11.9	11.9	6.9	166
378	16.4	9.4	1.1	11.9	11.9	6.8	166
379	16.2	9.4	0.9	11.8	11.8	6.8	166
380	16.4	9.5	0.8	11.8	11.8	6.8	166
381	15.9	9.6	0.7	11.8	11.8	6.8	166
382	14.9	9.4	0.4	11.9	12.0	6.8	166
383	13.5	9.1	0.1	12.2	12.0	6.8	166
384	11.5	8.5	-0.7	11.8	11.8	6.8	166
385	9.7	8.0	-1.5	11.8	11.8	6.8	166
386	8.9	7.5	-1.9	11.8	11.8	6.8	166
387	8.5	7.3	-2.0	11.9	11.9	6.8	166
388	8.4	7.2	-2.2	11.8	11.9	6.8	166
389	8.2	7.1	-2.3	12.1	12.0	6.8	166
390	8.3	7.0	-2.3	12.3	12.8	6.8	166
391	8.1	7.2	-2.0	12.1	12.0	6.8	166
392	8.3	7.5	-1.9	12.4	12.2	6.8	166
393	8.6	7.6	-1.9	11.9	11.8	6.8	166
394	8.9	7.9	-2.0	11.8	12.0	6.8	166
395	9.4	7.8	-2.1	11.8	11.8	6.8	166
396	9.7	7.6	-2.1	11.9	11.8	6.8	166
397	9.7	7.3	-2.1	11.9	11.9	6.8	166
398	9.3	6.9	-2.0	12.2	12.1	6.8	166
399	9.6	6.8	-2.0	11.9	11.9	6.8	166
400	9.6	6.8	-1.8	12.0	12.0	6.9	166

Depth (mm)	Axial Stress (MPa)	Hoop Stress (MPa)	Shear Stress (MPa)	Axial Error (MPa)	Hoop Error (MPa)	Shear Error (MPa)	Young's Modulus (GPa)
401	9.7	6.9	-1.9	11.9	11.8	6.8	166
402	9.7	6.8	-1.9	11.9	11.8	6.8	166
403	9.3	6.7	-1.9	11.8	11.8	6.8	166
404	9.4	6.8	-2.0	11.8	11.8	6.8	166
405	9.4	6.7	-2.2	11.9	11.9	6.8	166
406	9.0	6.6	-2.4	11.8	11.8	6.9	166
407	8.7	6.2	-2.7	11.9	11.8	6.8	166
408	8.6	6.1	-2.8	11.8	11.9	6.9	166
409	8.3	6.2	-3.0	11.9	11.8	6.8	166
410	7.2	5.8	-3.3	12.0	11.9	6.8	166
411	5.5	5.2	-3.8	11.8	11.9	6.8	166
412	4.5	5.0	-4.0	12.5	12.4	6.9	166
413	3.7	4.9	-3.4	12.8	12.6	6.8	166
414	2.8	5.0	-2.5	11.9	11.8	6.8	166
415	1.6	4.9	-1.5	18.9	18.0	7.0	166
416	1.9	4.4	-0.9	11.8	11.8	6.8	166
417	1.5	2.8	0.5	12.3	12.6	7.6	166
418	1.6	1.3	1.7	12.4	12.0	6.9	166
419	2.6	0.1	2.3	14.0	13.9	6.9	166
420	5.1	1.1	1.3	11.8	11.9	6.8	166
421	6.9	3.1	-0.1	11.8	12.0	6.8	166
422	8.2	5.1	-1.0	12.2	12.3	6.8	166
423	8.3	6.3	-1.5	12.3	12.6	6.8	166
424	8.3	6.9	-2.1	12.5	12.5	6.8	166
425	7.2	7.2	-2.7	12.6	12.9	6.9	166
426	7.0	7.2	-3.4	11.9	11.9	6.8	166
427	6.5	6.8	-3.9	11.9	12.0	6.8	166
428	5.7	6.7	-4.2	12.2	11.9	6.8	166
429	5.0	7.1	-4.4	11.8	11.9	6.8	166
430	4.6	7.1	-4.5	12.0	12.0	6.8	166
431	5.6	7.9	-4.3	11.8	11.8	6.8	166
432	7.1	9.1	-3.8	11.9	11.8	6.8	166
433	8.4	9.7	-3.4	11.9	12.0	6.9	166
434	9.1	10.3	-3.0	11.9	11.8	6.8	166
435	9.4	10.8	-2.8	12.1	12.1	6.8	166
436	9.9	11.3	-2.8	11.9	11.8	6.9	166
437	10.0	11.6	-2.8	12.0	11.9	6.8	166
438	9.9	11.9	-2.7	11.8	11.8	6.8	166
439	9.6	11.9	-3.0	11.9	11.9	6.9	166
440	9.3	11.6	-3.3	11.8	11.8	6.8	166
441	8.9	11.0	-3.8	11.8	11.8	6.8	166
442	8.9	11.2	-4.0	11.8	11.8	6.8	166
443	9.4	11.8	-3.8	11.8	11.8	6.8	166

Depth (mm)	Axial Stress (MPa)	Hoop Stress (MPa)	Shear Stress (MPa)	Axial Error (MPa)	Hoop Error (MPa)	Shear Error (MPa)	Young's Modulus (GPa)
444	10.1	12.3	-3.4	11.9	11.9	6.8	166
445	10.9	12.7	-3.1	12.0	11.8	6.9	166
446	11.9	12.8	-3.0	11.8	11.9	6.8	166
447	13.3	13.4	-2.5	11.8	11.8	6.9	166
448	15.2	14.1	-2.0	11.8	11.8	6.8	166
449	17.7	14.7	-1.1	11.9	11.8	6.8	166
450	20.2	15.2	-0.2	12.0	12.0	6.8	166
451	20.6	14.5	0.0	12.0	11.9	6.9	166
452	19.7	13.8	-0.3	12.0	12.0	6.9	166
453	18.0	14.6	-1.0	11.8	11.8	6.8	166
454	15.5	15.6	-1.6	11.8	12.0	6.8	166
455	13.3	16.2	-2.2	11.8	12.0	7.2	166
456	12.6	17.0	-2.7	12.4	12.2	6.8	166
457	12.9	17.9	-2.8	12.3	12.2	6.8	166
458	13.4	18.5	-3.0	11.8	11.9	6.8	166
459	13.5	19.0	-3.3	11.8	11.9	6.8	166
460	13.4	19.3	-3.4	11.9	12.0	6.8	166
461	13.2	19.8	-3.7	12.0	11.9	6.8	166
462	13.2	20.3	-4.0	11.9	11.9	6.8	166
463	13.3	20.7	-4.2	12.1	12.0	6.8	166
464	13.2	21.1	-4.3	11.8	11.8	6.8	166
465	13.2	21.5	-4.5	12.2	12.1	7.0	166
466	13.1	21.4	-4.4	12.1	12.1	6.8	166
467	12.2	20.8	-4.3	11.9	11.9	6.9	166
468	11.2	20.5	-4.6	11.8	11.9	6.8	166
469	10.0	20.1	-4.6	11.8	11.8	6.9	166
470	9.3	20.0	-4.3	11.9	12.0	6.8	166
471	9.4	20.2	-3.8	11.9	12.0	6.8	166
472	9.7	20.5	-3.2	12.0	11.9	6.8	166
473	9.9	20.8	-2.8	11.9	12.0	6.8	166
474	10.3	20.6	-2.7	11.8	11.9	6.8	166
475	10.1	20.3	-2.8	12.1	11.9	6.8	166
476	9.5	19.8	-2.9	12.0	11.9	6.8	166
477	9.2	18.9	-3.1	12.0	12.1	6.8	166
478	9.2	17.9	-3.0	11.8	11.9	6.9	166
479	9.7	16.9	-2.7	2.0	1.8	0.9	166
480	9.6	16.7	-2.3	11.9	11.9	6.8	166
481	8.8	16.7	-2.1	12.3	12.6	7.1	166
482	7.8	16.7	-2.0	12.3	12.3	7.0	166
483	7.5	17.0	-1.9	12.2	12.1	7.0	166
484	7.1	17.0	-1.5	12.5	12.4	7.0	166
485	6.5	17.2	-1.1	12.2	12.3	7.0	166
486	6.0	17.4	-1.3	12.4	12.4	7.0	166

Depth (mm)	Axial Stress (MPa)	Hoop Stress (MPa)	Shear Stress (MPa)	Axial Error (MPa)	Hoop Error (MPa)	Shear Error (MPa)	Young's Modulus (GPa)
487	5.8	17.2	-1.6	12.2	12.2	7.1	166
488	5.9	16.7	-1.4	12.3	12.3	7.1	166
489	6.2	16.3	-1.3	12.8	12.8	7.0	166
490	6.4	16.2	-1.2	12.4	12.7	7.0	166
491	6.3	15.8	-1.0	12.3	12.3	7.0	166
492	6.3	15.4	-1.1	12.2	12.2	7.0	166
493	6.6	14.8	-1.0	12.2	12.3	7.0	166
494	6.7	14.3	-0.8	12.3	12.6	7.1	166
495	6.7	14.1	-0.6	12.2	12.4	7.0	166
496	6.6	14.0	-0.5	12.2	12.2	7.0	166
497	6.5	13.7	-0.4	12.4	12.4	7.0	166
498	6.3	13.3	-0.4	12.3	12.4	7.2	166
499	5.9	12.8	-0.4	12.6	12.3	7.1	166
500	5.7	12.6	-0.5	12.2	12.2	7.0	166
501	5.9	12.6	-0.4	12.3	12.3	7.0	166
502	6.3	12.0	-0.2	12.3	12.3	7.0	166
503	6.6	11.5	-0.2	12.5	12.3	7.0	166
504	6.7	11.1	-0.1	12.3	12.4	7.0	166
505	6.9	10.6	-0.1	12.2	12.4	7.0	166
506	7.2	10.1	-0.3	12.3	12.5	7.1	166
507	7.7	9.6	-0.1	12.2	12.3	7.0	166
508	7.6	8.8	0.1	12.2	12.2	7.0	166
509	7.3	7.5	0.4	12.3	12.2	7.0	166
510	6.7	5.8	0.7	12.2	12.2	7.0	166
511	5.8	4.2	1.0	12.3	12.2	7.0	166
512	5.0	2.8	0.9	12.2	12.2	7.0	166

Table 4: DHD measured residual stress results for the measurement 4 location (reduced data set).

Depth (mm)	Axial Stress (MPa)	'Hoop' Stress (MPa)	Shear Stress (MPa)	Axial Error (MPa)	'Hoop' Error (MPa)	Shear Error (MPa)	Young's Modulus (GPa)
0.0-0.8	Omitted due to free surfaces						N/A
1	-37.7	-35.3	-4.2	20.5	20.1	8.7	166
2	-20.4	-24.5	-1.7	13.0	13.1	6.7	166
3	-4.0	-11.5	-3.1	11.9	11.6	6.8	166
4	2.5	-6.6	-1.6	12.8	12.5	6.6	166
5	5.0	-4.9	-4.8	13.4	13.5	6.9	166
6	8.2	-1.1	-6.4	11.8	11.9	6.7	166
7	8.5	0.8	-6.9	11.5	11.9	6.6	166
8	9.9	3.1	-8.2	12.5	11.6	6.6	166
9	11.3	5.5	-7.4	12.3	11.9	6.9	166
10	10.5	4.6	-7.7	12.0	12.0	6.7	166

Depth (mm)	Axial Stress (MPa)	'Hoop' Stress (MPa)	Shear Stress (MPa)	Axial Error (MPa)	'Hoop' Error (MPa)	Shear Error (MPa)	Young's Modulus (GPa)
11	8.3	3.6	-6.7	11.8	11.8	6.7	166
12	5.8	1.0	-5.8	11.7	12.0	6.6	166
13	6.8	5.0	-6.6	11.5	11.4	6.6	166
14	4.4	3.4	-6.8	11.6	11.8	6.7	166
15	-0.5	-0.6	-7.3	11.5	11.6	6.8	166
16	-2.2	-1.4	-7.3	11.4	11.6	6.7	166
17	-4.9	-4.8	-6.3	11.6	11.7	6.7	166
18	-5.8	-5.5	-7.1	11.6	11.5	6.7	166
19	-8.0	-9.5	-7.0	11.6	11.5	6.7	166
20	-10.9	-13.9	-6.6	11.7	11.5	6.7	166
21	-11.9	-16.1	-6.4	11.8	11.9	6.8	166
22	-16.0	-19.4	-7.0	11.6	11.8	6.6	166
23	-16.2	-20.6	-7.8	11.5	11.5	6.7	166
24	-17.7	-22.6	-7.5	12.0	11.6	6.8	166
25	-17.5	-21.9	-7.5	12.0	12.1	6.8	166
26	-15.8	-21.9	-7.5	11.5	11.7	6.7	166
27	-15.8	-22.4	-5.8	11.6	11.5	6.6	166
28	-15.0	-20.9	-6.6	11.8	11.7	6.7	166
29	-15.5	-20.0	-6.6	12.2	12.4	6.6	166
30	-15.0	-19.6	-6.9	11.6	11.9	6.7	166
31	-16.1	-19.6	-7.0	11.5	11.5	6.6	166
32	-16.4	-20.3	-6.5	11.9	11.9	6.6	166
33	-15.5	-17.8	-7.3	13.2	13.5	6.7	166
34	-15.4	-17.5	-6.5	13.2	12.9	6.7	166
35	-16.7	-17.9	-6.0	11.7	11.8	6.6	166
36	-13.5	-14.8	-7.2	12.1	11.7	6.6	166
37	-16.2	-18.5	-6.4	13.4	13.4	6.6	166
38	-14.3	-16.6	-7.0	13.6	13.7	6.6	166
39	-12.8	-14.3	-6.7	12.3	12.0	6.6	166
40	-13.6	-15.6	-6.1	11.7	11.5	6.6	166
41	-14.6	-15.1	-6.9	11.9	11.7	6.6	166
42	-13.7	-15.1	-6.0	12.3	12.2	6.6	166
43	-15.1	-14.9	-6.3	11.6	11.6	6.6	166
44	-14.6	-14.6	-6.5	11.5	11.5	6.7	166
45	-16.4	-15.2	-5.3	11.7	11.9	6.6	166
46	-15.2	-14.5	-6.5	11.9	11.7	6.6	166
47	-15.8	-13.8	-6.5	11.5	11.6	6.6	166
48	-17.8	-15.2	-5.9	11.4	11.6	6.6	166
49	-15.3	-12.6	-6.7	11.7	11.9	6.9	166
50	-15.5	-13.3	-6.6	11.9	11.5	6.8	166
51	-14.1	-11.9	-6.9	11.8	11.5	6.6	166
52	-13.7	-10.2	-6.8	12.5	12.2	6.7	166
53	-13.5	-10.5	-7.0	11.7	11.8	6.8	166

Depth (mm)	Axial Stress (MPa)	'Hoop' Stress (MPa)	Shear Stress (MPa)	Axial Error (MPa)	'Hoop' Error (MPa)	Shear Error (MPa)	Young's Modulus (GPa)
54	-14.2	-10.6	-6.5	11.5	11.7	6.6	166
55	-15.3	-10.8	-6.0	11.4	11.4	6.6	166
56	-15.2	-9.8	-6.0	11.5	11.5	6.7	166
57	-15.5	-8.4	-6.2	11.5	11.6	6.6	166
58	-15.3	-9.9	-6.1	11.5	11.5	6.7	166
59	-14.9	-9.8	-5.2	11.8	11.7	6.6	166
60	-15.9	-9.5	-5.3	12.2	12.3	6.6	166
61	-15.9	-10.4	-4.3	12.0	12.0	6.7	166
62	-15.8	-8.8	-3.4	11.5	11.7	6.6	166
63	-15.4	-7.9	-4.6	11.5	12.0	6.7	166
64	-15.7	-7.7	-4.5	11.5	11.6	6.6	166
65	-14.9	-6.1	-5.1	11.8	11.5	6.6	166
66	-15.1	-7.3	-4.3	11.7	11.7	6.6	166
67	-15.1	-6.6	-5.1	11.8	11.9	6.7	166
68	-14.7	-5.6	-6.3	11.4	11.5	6.6	166
69	-15.1	-5.5	-5.3	11.5	11.5	6.6	166
70	-15.5	-5.6	-5.6	12.2	12.0	6.7	166
71	-14.4	-4.4	-5.8	11.9	11.8	6.6	166
72	-15.1	-3.2	-6.3	11.7	11.7	6.7	166
73	-13.8	-2.7	-6.0	11.5	11.6	6.6	166
74	-13.9	-3.6	-5.2	11.6	11.5	6.7	166
75	-13.7	-3.1	-5.6	11.9	11.8	6.6	166
76	-12.3	-2.0	-6.4	12.2	12.2	6.7	166
77	-13.4	-4.2	-6.2	11.5	11.5	6.6	166
78	-13.8	-5.4	-6.7	11.9	11.8	6.6	166
79	-15.9	-8.9	-6.7	11.9	11.5	6.6	166
80	-17.1	-12.3	-7.4	11.7	11.5	6.6	166
81	-18.1	-14.7	-7.4	11.5	11.6	6.7	166
82	-23.6	-16.4	-6.1	11.5	11.6	6.7	166
83	-26.5	-15.3	-6.4	12.2	11.4	6.9	166
84	-34.2	-20.6	-7.1	11.4	11.4	6.7	166
85	Omitted due to free surfaces						N/A
86							N/A
87							N/A
88							N/A
89							N/A
90							N/A
91							N/A
92	61.3	-24.6	-5.6	16.5	14.6	8.5	210
93	67.5	-18.1	-4.2	16.3	16.3	8.5	210
94	65.3	-19.3	0.5	15.1	15.0	8.4	210
95	66.9	-16.8	0.8	14.7	14.6	8.3	210
96	69.0	-16.0	0.3	14.7	14.5	8.3	210

Depth (mm)	Axial Stress (MPa)	'Hoop' Stress (MPa)	Shear Stress (MPa)	Axial Error (MPa)	'Hoop' Error (MPa)	Shear Error (MPa)	Young's Modulus (GPa)
97	69.2	-18.0	3.8	15.0	15.0	8.3	210
98	68.6	-18.3	4.2	16.1	16.0	8.4	210
99	67.9	-17.1	4.3	15.0	14.8	8.3	210
100	68.3	-11.6	7.3	14.6	14.8	8.6	210
101	67.3	-14.1	4.9	14.7	14.8	8.6	210
102	66.2	-13.3	5.2	15.2	15.4	8.4	210
103	66.9	-10.6	5.0	14.8	14.8	8.4	210

Table 5: DHD measured residual stress results for the measurement 5 location (reduced data set).

Depth (mm)	Axial Stress (MPa)	'Hoop' Stress (MPa)	Shear Stress (MPa)	Axial Error (MPa)	'Hoop' Error (MPa)	Shear Error (MPa)	Young's Modulus (GPa)
0.0-0.8	Omitted due to free surfaces						N/A
1	50.5	39.2	-27.9	26.9	29.0	14.8	210
2	64.6	39.8	-27.9	32.4	32.0	14.9	210
3	77.1	40.6	-24.7	26.4	26.2	14.7	210
4	86.4	34.0	-22.9	25.8	25.8	14.6	210
5	87.5	29.2	-19.6	25.5	25.4	14.7	210
6	81.9	25.5	-12.7	25.8	25.7	14.6	210
7	80.4	13.6	-12.2	25.8	25.4	14.7	210
8	73.3	-1.3	-5.1	28.0	26.5	15.8	210
9	66.8	-1.5	-3.7	26.3	26.5	14.7	210
10	Omitted due to free surfaces						N/A
11							N/A
12	-10.9	20.0	-3.8	21.9	19.8	11.3	166
13	-6.7	23.1	-0.9	19.6	19.5	11.3	166
14	-2.8	24.9	-0.1	20.0	19.9	11.3	166
15	-2.4	25.2	-0.8	19.6	19.8	11.3	166
16	-1.8	23.9	-1.8	19.7	20.0	11.5	166
17	-1.4	23.5	-2.1	19.6	19.7	11.3	166
18	-3.1	21.8	-2.3	19.4	19.4	11.4	166
19	-4.0	19.9	-2.3	19.5	19.4	11.3	166
20	-2.7	20.1	-2.2	19.6	19.5	11.3	166
21	-2.1	19.8	-2.4	19.6	19.7	11.4	166
22	-0.8	22.7	-0.3	19.5	19.5	11.3	166
23	-0.8	22.0	-1.0	19.5	19.7	11.3	166
24	-0.2	20.7	0.3	19.5	19.8	11.3	166
25	-3.4	19.3	-0.1	19.6	19.5	11.3	166
26	-2.8	20.2	-0.9	19.6	19.7	11.3	166
27	-3.2	21.3	-1.3	19.4	19.6	11.2	166
28	-3.3	20.6	-0.9	19.5	19.5	11.2	166
29	-7.1	19.6	0.3	19.4	19.5	11.3	166

Depth (mm)	Axial Stress (MPa)	'Hoop' Stress (MPa)	Shear Stress (MPa)	Axial Error (MPa)	'Hoop' Error (MPa)	Shear Error (MPa)	Young's Modulus (GPa)
30	-2.1	20.8	-0.1	19.5	19.5	11.3	166
31	-1.3	19.5	-0.2	19.5	19.4	11.4	166
32	-1.6	16.5	1.7	19.7	19.8	11.2	166
33	-4.0	16.6	3.3	19.6	19.9	11.3	166
34	-2.7	16.8	1.3	19.5	19.8	11.2	166
35	-4.1	17.9	1.0	19.5	19.7	11.5	166
36	-3.9	16.1	1.3	19.9	19.8	11.3	166
37	-2.1	16.5	1.7	19.6	19.9	11.2	166
38	-1.9	18.7	1.8	19.4	19.6	11.2	166
39	-2.6	19.9	1.6	19.5	19.6	11.2	166
40	-1.8	18.5	0.4	19.5	19.6	11.3	166
41	-2.0	18.6	0.0	19.6	19.5	11.2	166
42	-0.9	18.1	0.1	19.4	19.5	11.2	166
43	-1.6	18.7	0.1	19.4	19.4	11.2	166
44	-0.1	20.2	0.3	19.4	19.4	11.2	166
45	-0.7	21.0	-0.7	19.5	19.7	11.2	166
46	-1.1	18.6	-0.1	19.5	19.5	11.2	166
47	0.2	17.6	0.8	19.4	19.5	11.2	166
48	-1.3	17.8	1.2	19.4	19.6	11.2	166
49	-1.7	18.2	0.6	19.4	19.4	11.3	166
50	-0.1	18.8	1.3	19.5	19.5	11.2	166
51	1.2	18.6	2.2	19.8	20.2	11.3	166
52	2.5	17.3	2.8	19.6	19.7	11.3	166
53	3.1	19.1	4.0	19.6	19.8	11.2	166
54	3.5	20.2	3.1	19.6	19.5	11.3	166
55	3.2	19.9	3.9	19.4	19.6	11.2	166
56	4.4	23.8	4.2	19.6	19.5	11.2	166
57	4.2	20.9	2.9	19.4	19.4	11.2	166
58	4.8	24.3	0.6	19.5	19.7	11.3	166
59	1.5	25.8	1.8	19.5	19.5	11.2	166
60	1.1	24.8	3.3	19.4	19.4	11.2	166
61	1.8	26.6	1.9	19.5	19.6	11.2	166
62	1.1	27.5	1.9	19.5	19.6	11.2	166
63	0.1	28.8	3.0	19.6	19.5	11.3	166
64	-3.1	27.2	1.2	19.5	19.4	11.2	166
65	-3.8	27.9	1.5	19.4	19.4	11.3	166
66	-1.6	32.8	2.2	19.4	19.5	11.6	166
67	0.3	33.5	2.0	19.5	19.7	11.4	166
68	3.4	33.1	0.2	19.4	19.4	11.2	166
69	2.2	31.2	0.4	19.4	19.6	11.3	166
70	1.5	32.7	0.7	19.5	19.7	11.3	166
71	4.4	31.5	0.3	19.5	19.5	11.3	166
72	-2.7	26.6	4.4	19.7	20.2	11.4	166

Depth (mm)	Axial Stress (MPa)	'Hoop' Stress (MPa)	Shear Stress (MPa)	Axial Error (MPa)	'Hoop' Error (MPa)	Shear Error (MPa)	Young's Modulus (GPa)
73	Omitted due to free surfaces						N/A
74							N/A
75	59.0	8.4	-16.1	27.1	25.5	12.7	210
76	61.2	15.6	-10.8	22.2	22.1	12.6	210
77	66.3	20.7	-7.1	24.9	24.0	12.9	210
78	69.3	28.5	-3.8	24.5	22.4	12.9	210
79	69.4	34.8	-1.2	22.1	21.9	12.6	210
80	71.3	40.4	3.0	23.3	23.2	12.7	210
81	66.7	39.4	5.0	22.5	22.3	12.7	210
82	53.4	38.6	5.6	22.1	21.9	12.6	210
83	33.7	34.2	7.9	24.4	22.1	12.7	210

Table 6: DHD measured residual stress results for the incorrect measurement location (reduced data set).

Depth (mm)	Axial Stress (MPa)	'Hoop' Stress (MPa)	Shear Stress (MPa)	Axial Error (MPa)	'Hoop' Error (MPa)	Shear Error (MPa)	Young's Modulus (GPa)
0.0-0.8	Omitted due to free surfaces						N/A
1	-59.1	-31.3	-10.3	13.0	15.7	7.3	166
2	-23.9	-5.7	-3.7	12.8	12.1	7.0	166
3	4.7	12.2	-1.0	12.1	12.2	6.9	166
4	20.3	28.1	-2.3	12.3	12.2	6.9	166
5	33.6	39.7	-5.4	12.1	12.2	6.9	166
6	22.2	26.1	-0.7	12.2	12.4	6.8	166
7	16.0	18.3	-1.0	11.9	11.8	6.9	166
8	14.6	16.9	-2.1	12.2	12.8	7.0	166
9	18.4	20.9	-2.6	11.8	12.0	6.8	166
10	16.1	22.2	-0.6	11.9	12.2	6.9	166
11	17.3	26.4	-1.9	12.8	12.7	6.9	166
12	15.0	21.5	-0.5	12.2	12.0	7.0	166
13	17.0	18.3	-1.2	11.8	11.9	6.9	166
14	16.3	21.5	-2.8	11.8	11.8	7.0	166
15	15.3	23.9	-3.7	12.0	12.7	6.9	166
16	12.4	19.8	-3.4	11.8	12.1	6.8	166
17	7.0	12.8	-4.2	12.0	12.7	6.9	166
18	3.5	11.5	-3.9	11.9	12.0	6.9	166
19	2.9	10.7	-3.9	11.9	11.9	6.9	166
20	-1.2	1.7	0.7	12.5	12.4	6.8	166
21	-6.0	-0.1	2.8	11.8	11.8	6.9	166
22	-6.9	-3.9	3.1	11.8	11.8	6.8	166
23	-10.2	-6.1	3.5	11.8	11.8	6.9	166
24	-10.3	-9.0	3.2	12.3	12.1	6.9	166
25	-9.2	-7.9	3.3	11.9	11.8	6.9	166

Depth (mm)	Axial Stress (MPa)	'Hoop' Stress (MPa)	Shear Stress (MPa)	Axial Error (MPa)	'Hoop' Error (MPa)	Shear Error (MPa)	Young's Modulus (GPa)
26	-7.1	-7.2	2.2	11.8	11.8	7.0	166
27	-8.5	-8.9	3.7	11.8	11.8	6.8	166
28	-7.2	-5.8	2.5	11.9	12.0	6.8	166
29	-8.9	-5.8	1.2	11.8	12.0	6.9	166
30	-8.2	-0.4	0.5	11.9	11.8	6.9	166
31	-5.6	-4.3	1.6	12.2	12.0	6.8	166
32	-2.6	-5.1	2.9	12.0	12.0	6.8	166
33	1.0	0.9	0.8	12.0	11.8	6.8	166
34	1.6	-0.2	-0.4	12.1	12.0	6.8	166
35	-1.0	-2.3	-1.2	12.0	11.9	7.0	166
36	-1.7	-1.5	-2.1	11.9	12.2	6.9	166
37	-3.3	-2.9	-0.8	12.1	12.1	6.8	166
38	-5.3	-4.5	0.2	12.1	12.1	6.8	166
39	-5.8	-7.1	0.8	11.8	11.8	6.8	166
40	-5.0	-7.9	0.9	11.8	11.8	6.9	166
41	-6.2	-9.9	1.9	12.0	11.8	7.0	166
42	-10.4	-11.1	3.1	11.9	12.1	6.8	166
43	-12.8	-12.6	3.5	12.1	11.8	6.9	166
44	-13.5	-13.2	3.5	11.8	11.8	6.9	166
45	-14.3	-10.4	3.6	11.8	13.2	6.9	166
46	-8.8	-3.0	0.9	12.0	12.4	7.5	166

9 FIGURES

Figure 1: A photograph of the cast iron insert specimen delivered to VEQTER Ltd.

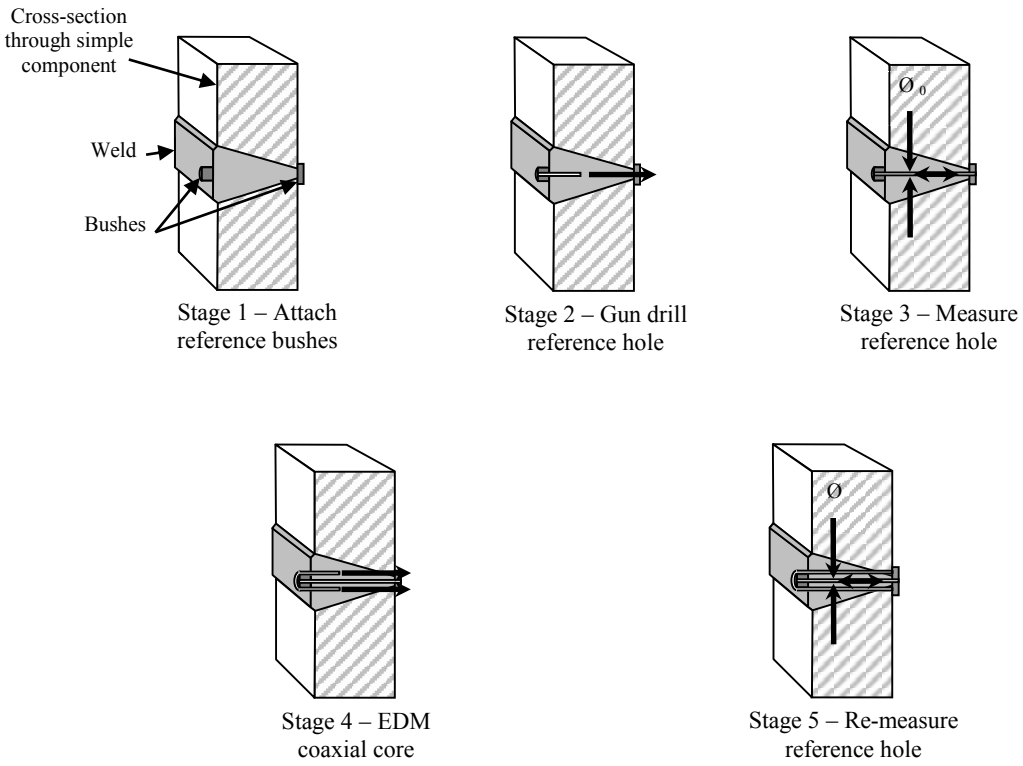

Figure 2: A schematic of the five stages involved in the DHD procedure.

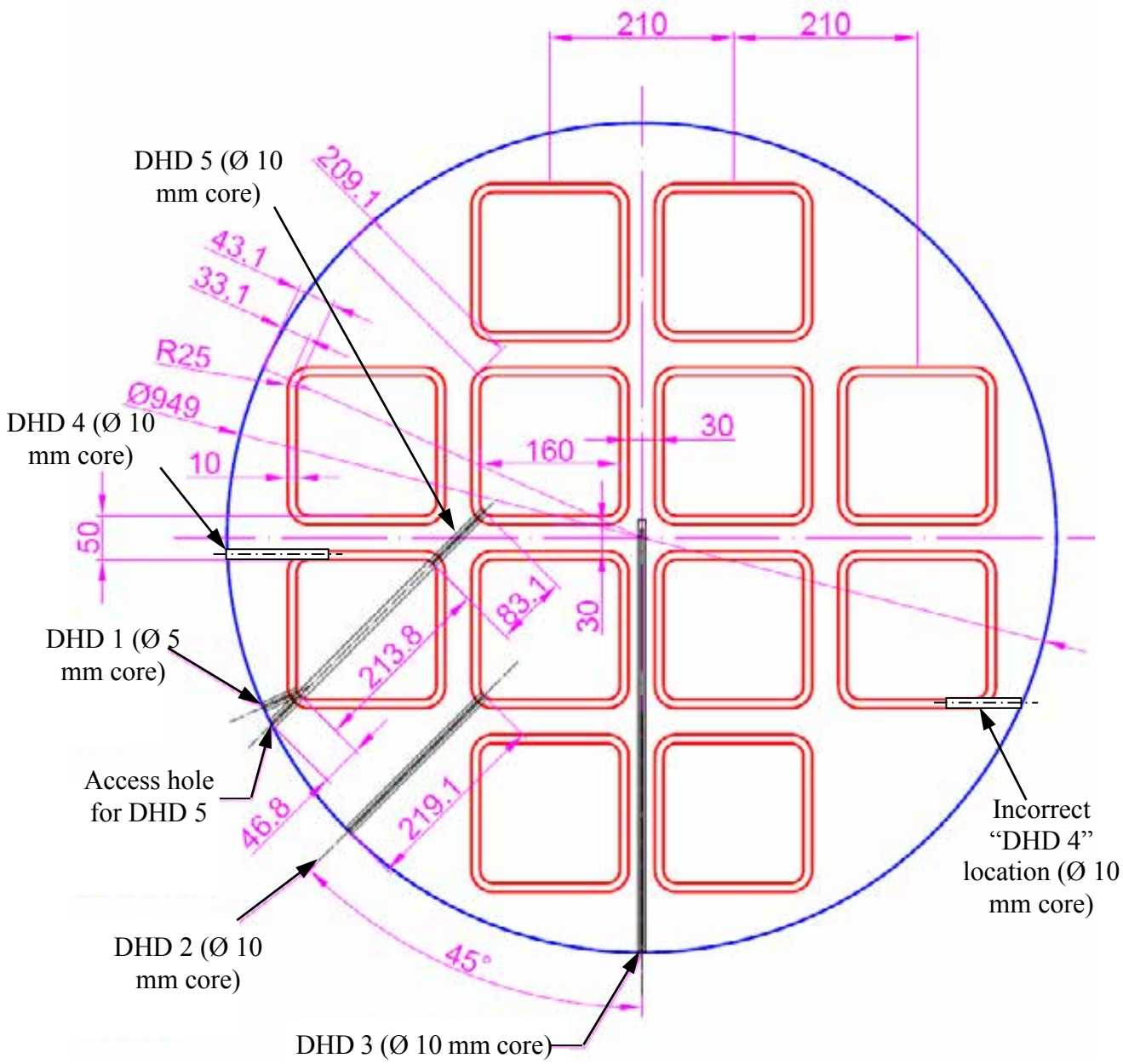

Figure 3: A cross sectional drawing of a similar cast iron insert specimen after final machining, illustrating all measurement locations (dimensions in mm).

Figure 4: A photograph showing the actual measurement locations performed in the specimens 'upper half' as it stood.

Figure 5: A photograph of the cores removed from the location 1 measurement.

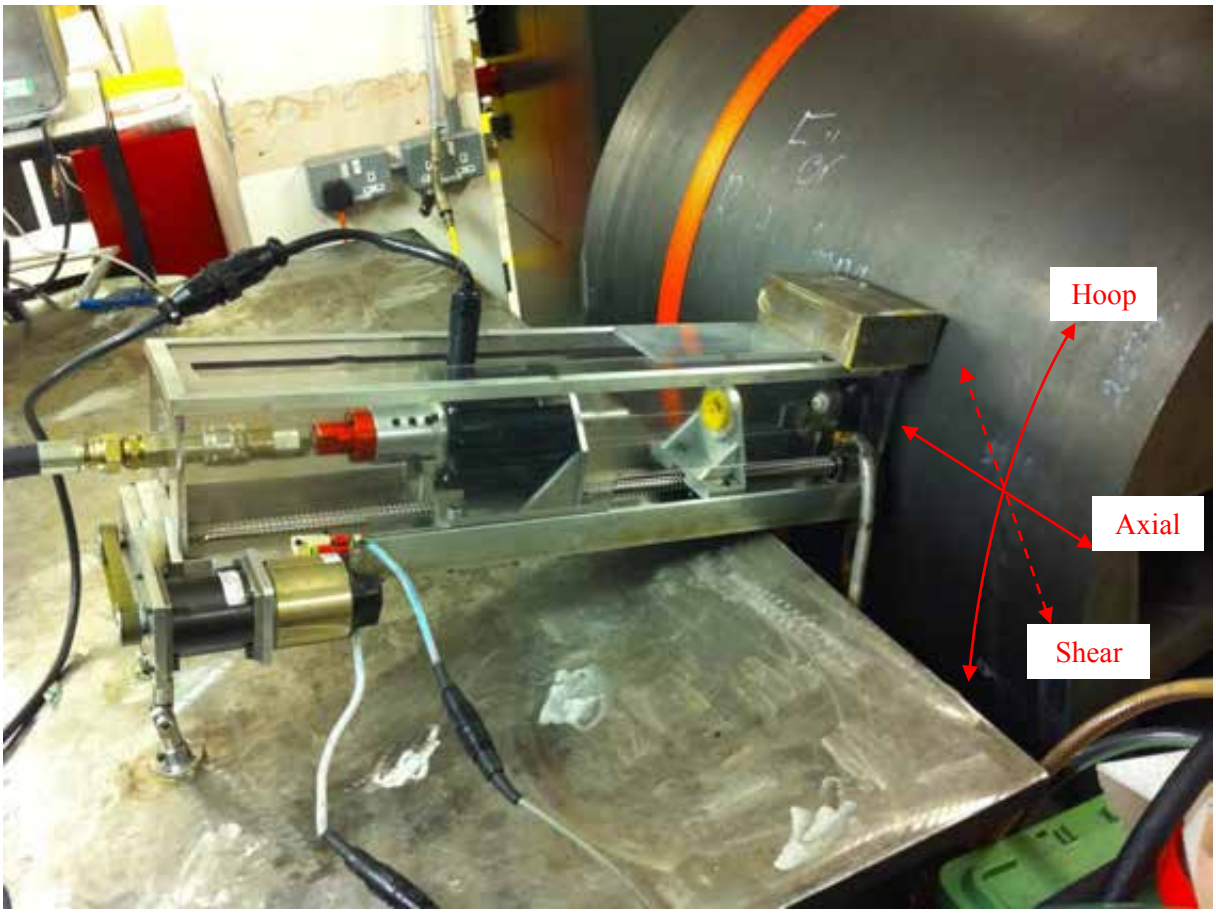

Figure 6: An image of the DHD machine during the gundrilling of measurement 1 with axes orientation illustrated.

Figure 7: A photograph of the 3 mm cores removed from the location 2 measurement.

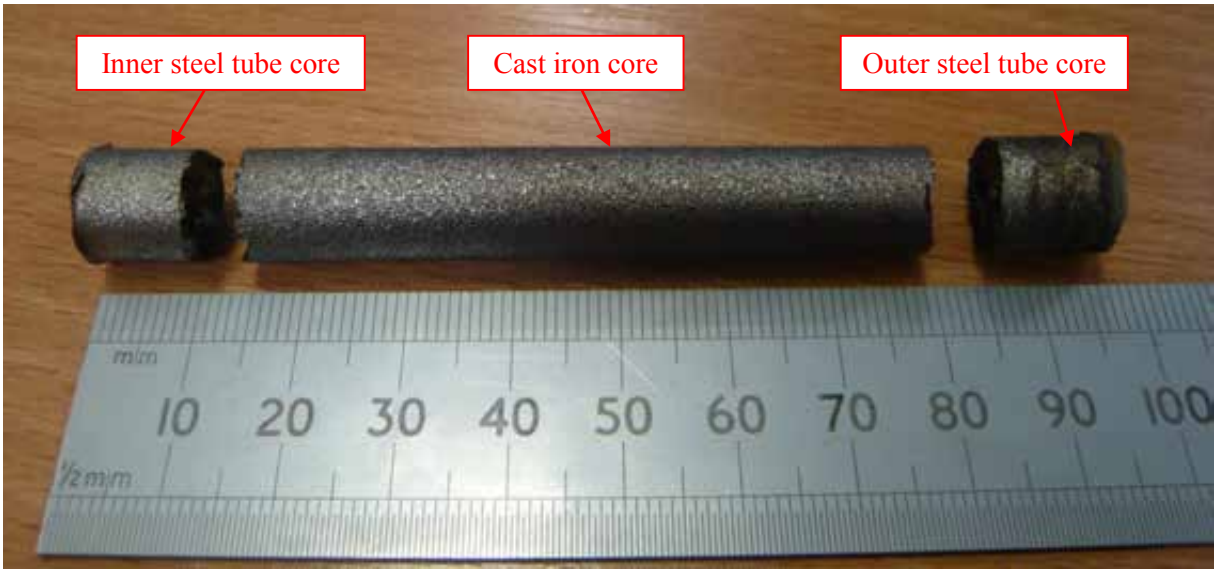

Figure 8: A photograph of the 3 mm cores removed from the location 5 measurement.

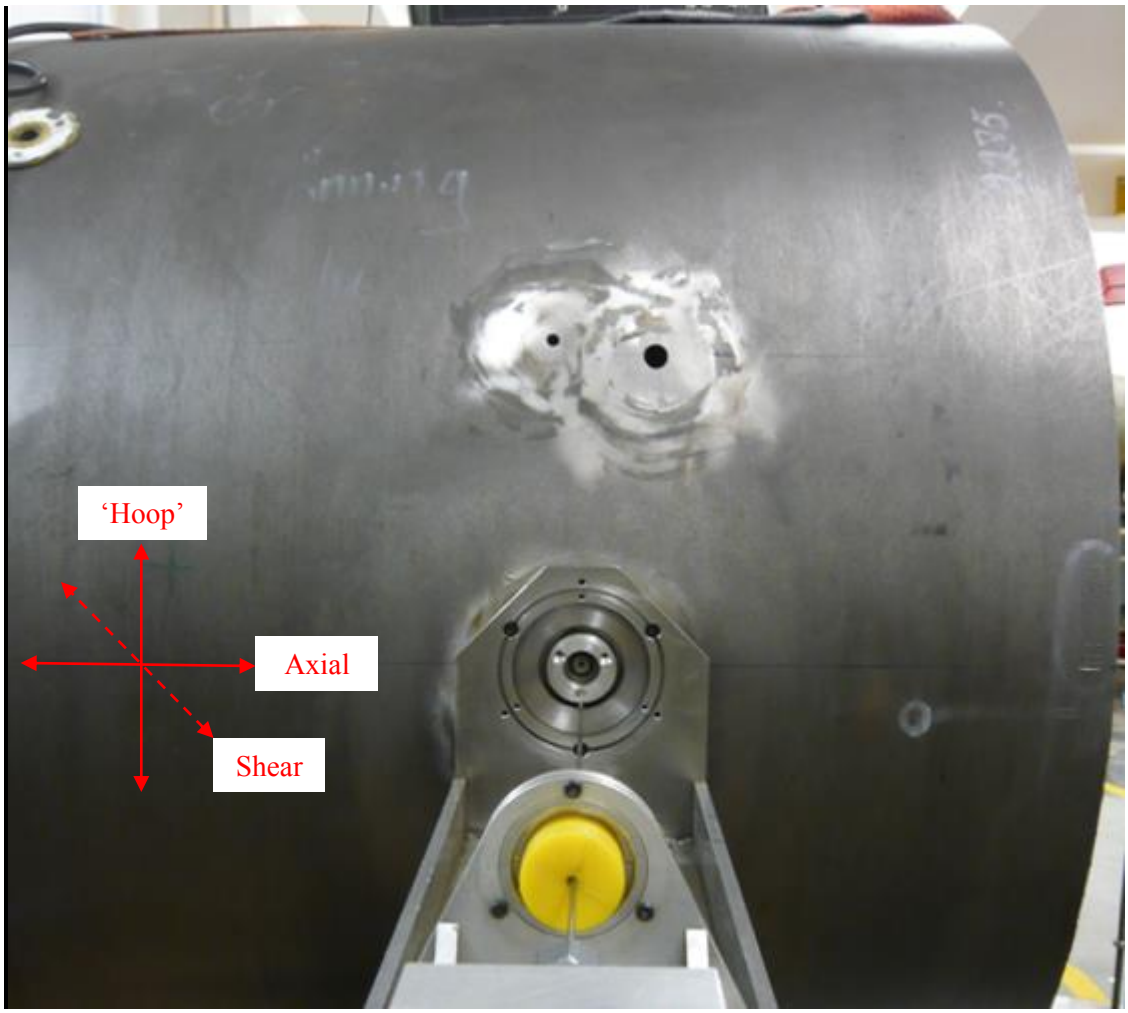

Figure 9: An image of the DHD machine during air probing at measurement 4 after stress relief, with axes orientation illustrated.

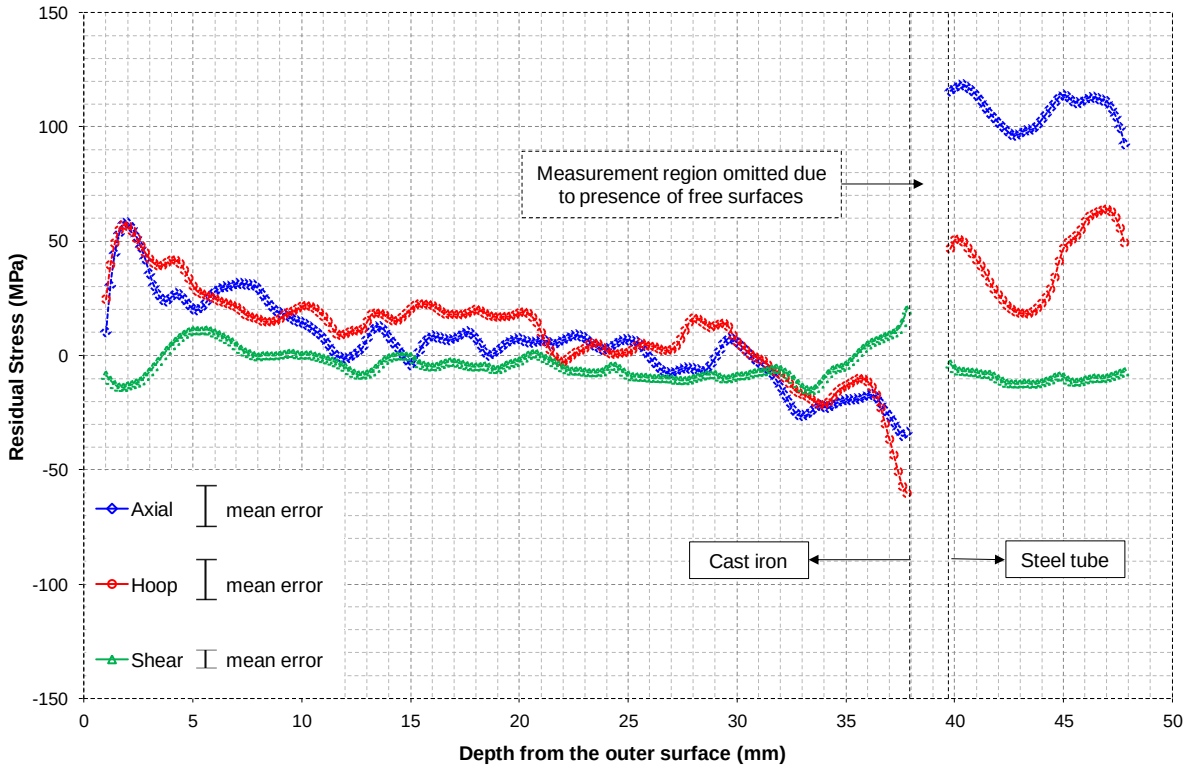

Figure 10: A graph showing residual stresses at the measurement 1 location.

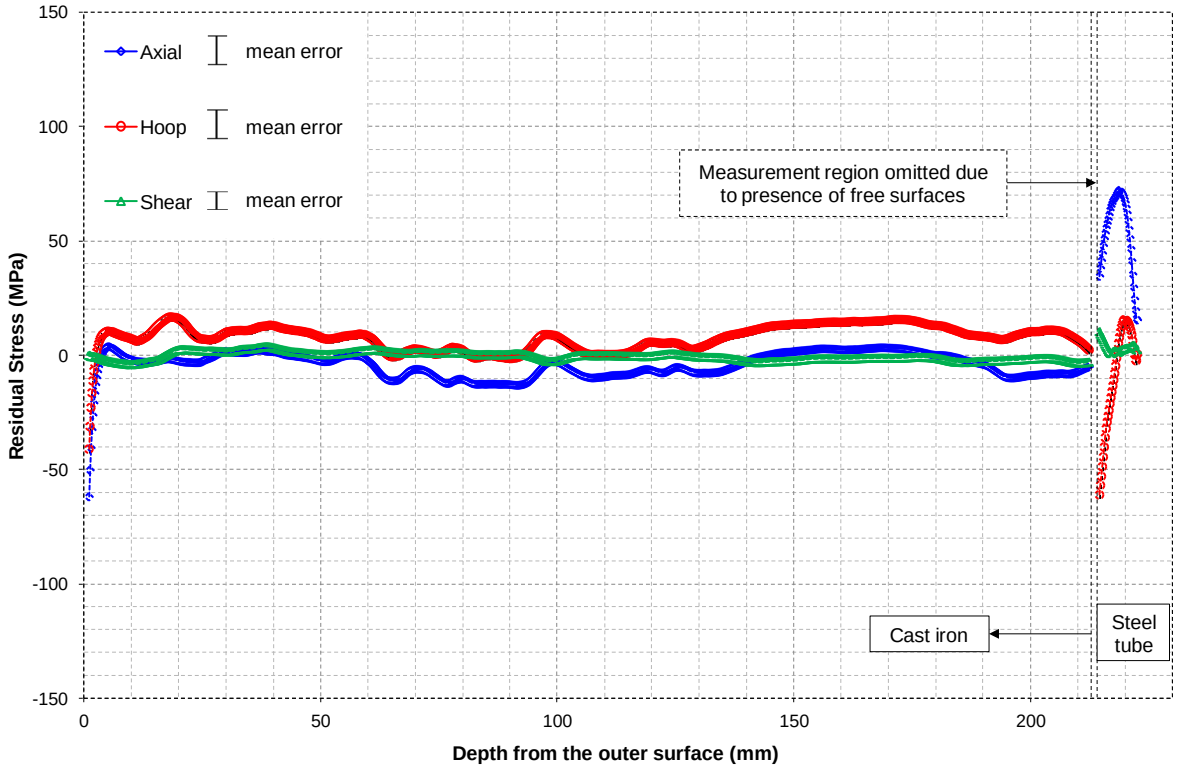

Figure 11: A graph showing residual stresses at the measurement 2 location.

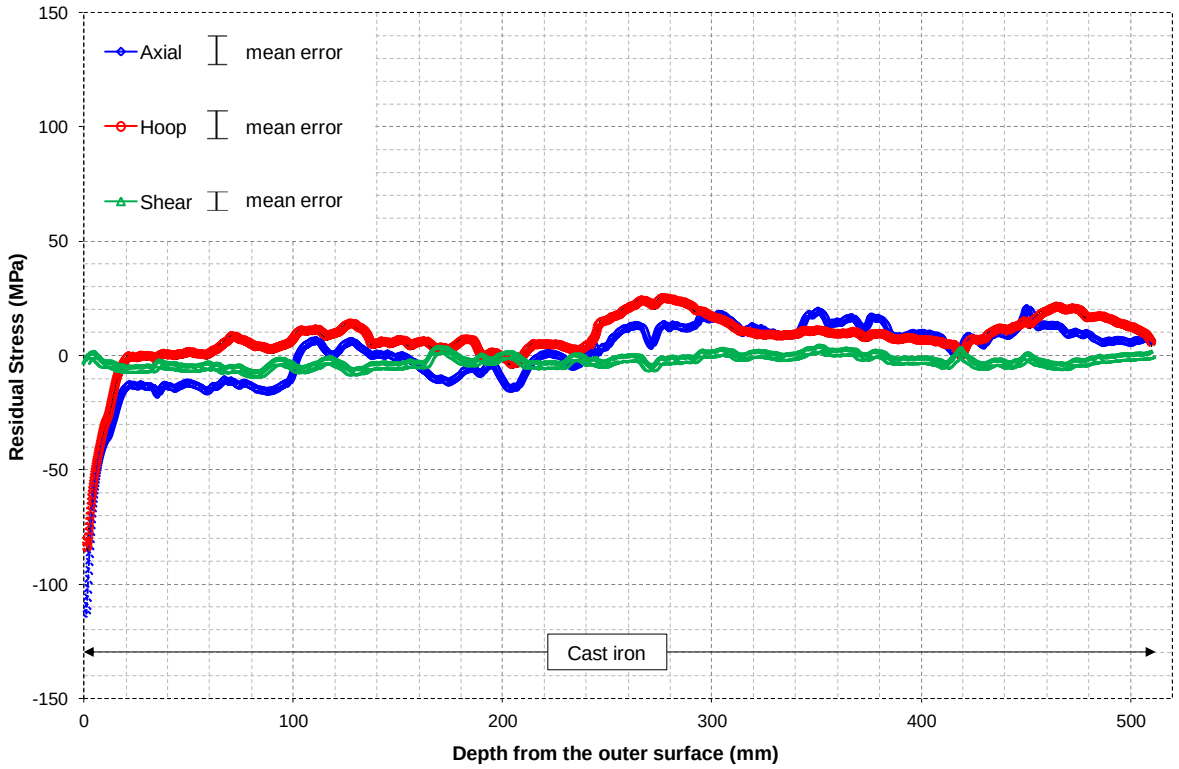

Figure 12: A graph showing residual stresses at the measurement 3 location.

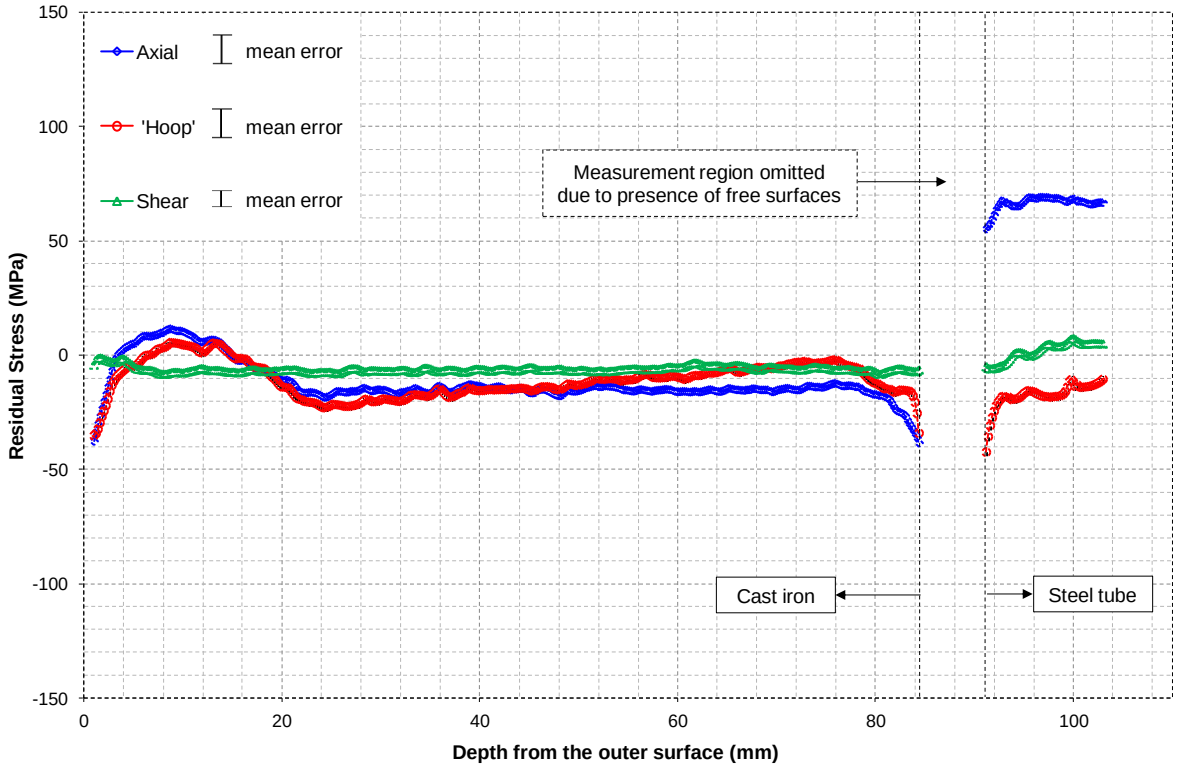

Figure 13: A graph showing residual stresses at the measurement 4 location.

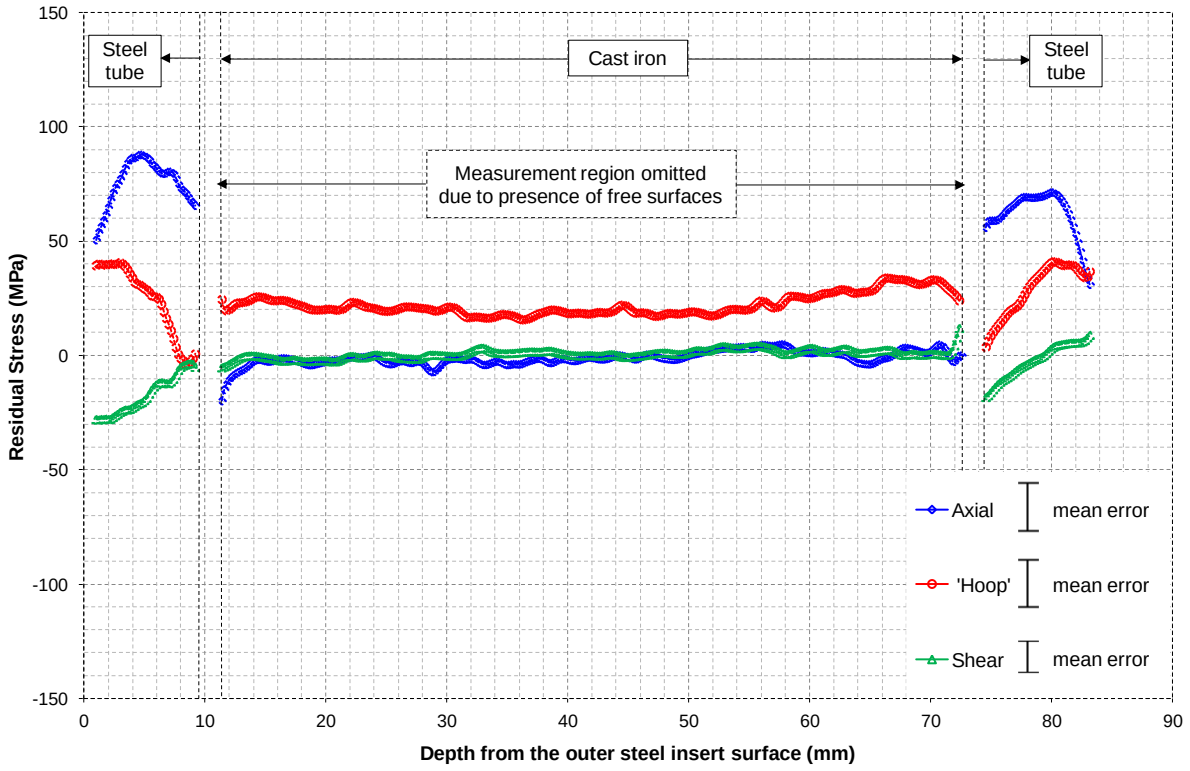

Figure 14: A graph showing residual stresses at the measurement 5 location.

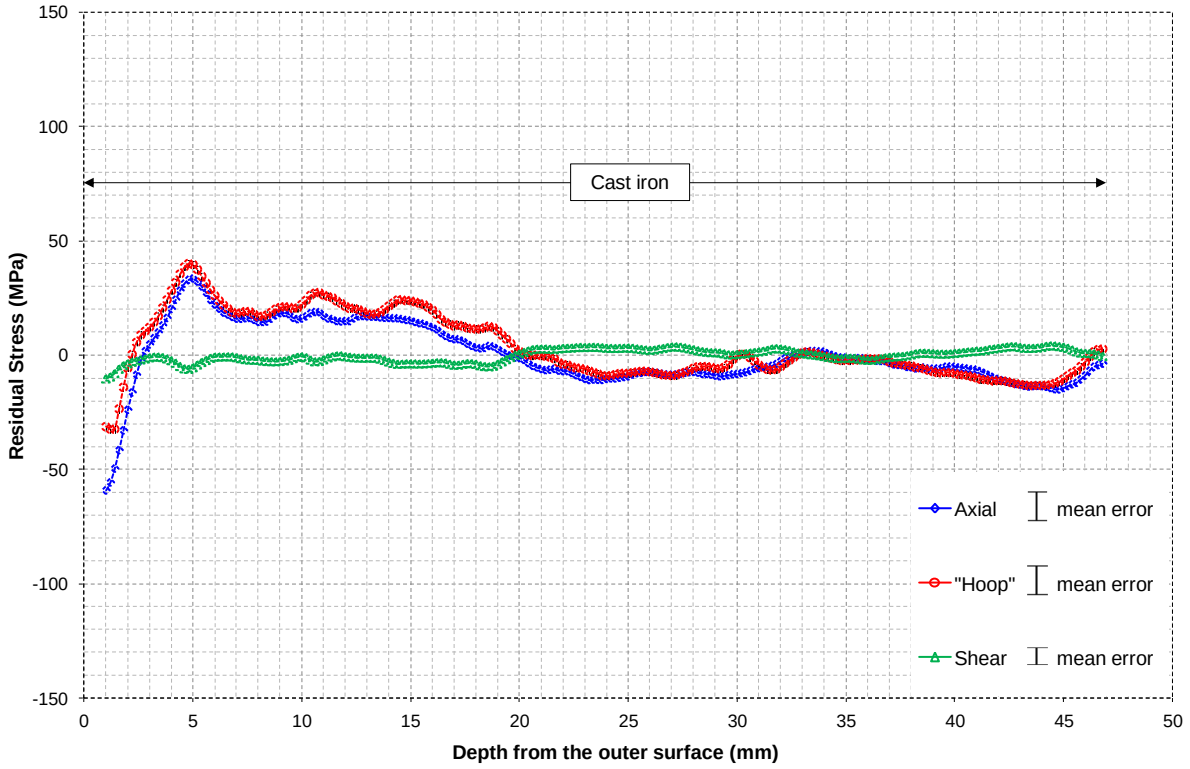

Figure 15: A graph showing residual stresses at the incorrect measurement location.